

1 Reguera-Rouzaud Nicole¹, Díaz-Viloria Noe^{1*}, Sánchez-Velasco Laura¹, Flores-
2 Morales Ana Laura², Parés-Sierra Alejandro³, Aburto-Oropeza, Octavio⁴, Munguía-
3 Vega Adrián^{5, 6}

4 **Yellow snapper (*Lutjanus argentiventris*) connectivity in the Southern Gulf of**
5 **California**

6
7 ¹Instituto Politécnico Nacional–Centro Interdisciplinario de Ciencias Marinas (IPN-
8 CICIMAR), Departamento de Plancton y Ecología Marina, La Paz, B.C.S., 23096,
9 Mexico.

10 ²Departamento de Oceanografía Física, Facultad de Ciencias Marinas,
11 Universidad Autónoma de Baja California, Ensenada, B.C., 22860, Mexico.

12 ³Departamento de Oceanografía Física, Centro de Investigación Científica y de
13 Educación Superior de Ensenada, Ensenada, B.C., 22860, Mexico.

14 ⁴Marine Biology Research Division, Scripps Institution of Oceanography, University
15 of California, San Diego, La Jolla, CA 92093-0202, USA.

16 ⁵Conservation Genetics Laboratory, School of Natural Resources and the
17 Environment, University of Arizona, Tucson, AZ, 85721, USA

18 ⁶@ Lab Applied Genetics Research. La Paz, Baja California Sur, 23000, Mexico

19 *Corresponding author: Tel. +52 (612) 122-5366, Ext. 81567; Fax: +52 (612) 122-
20 5322, ndviloria@hotmail.com

21

1 **Abstract**

2 We analysed the genetic connectivity and larval transport routes of *Lutjanus*
3 *argentiventris* to test if eddies could transport coastal-demersal fish larvae between
4 the peninsular and mainland coasts of the Southern Gulf of California. Larval
5 transport was estimated using the ROMS oceanographic model during the main
6 spawning period (July-August). We used 12 microsatellite loci to assess genetic
7 diversity, population structure and gene flow estimates in 233 *L. argentiventris*
8 samples from nine sites. The oceanographic model suggested the existence of a
9 stream flow and eddies that maintain connectivity in the Southern Gulf of
10 California. The global AMOVA and paired F_{ST} showed no significant genetic
11 differentiation among the sites, and the estimations of the number of migrants
12 indicated moderate to high gene flow among locations. However, after testing five
13 demographic scenarios of connectivity with a coalescent sampler, our results
14 supported the presence of a metapopulation structure with source-sink dynamics.
15 We discuss the challenges to reconcile our results considering the assumptions of
16 the different analyses and the characteristics of marine metapopulations.
17 Connectivity of *L. argentiventris* could be representative of other coastal-demersal
18 species with a similar life history and spawning season.

19 **Key words:** microsatellite, oceanographic model, larval dispersal, gene flow

20 **Acknowledgments**

21 This research was supported by grants from Consejo Nacional de Ciencia y
22 Tecnología (CONACyT) to Noé Díaz-Viloria (CB2015-257019) and Laura Sánchez-

1 Velasco (CB2014-236864-T), Secretaría de Investigación y posgrado del Instituto
2 Politécnico Nacional (IPN-SIP) to Noé Díaz-Viloria (20160514, 20170290,
3 20180339, 20195461) , and support from The David and Lucile Packard
4 Foundation to Adrián Munguía-Vega. Nicole Reguera-Rouzaud was a recipient of a
5 BEIFI-IPN and a CONACyT scholarship (No. 589502). We thank Ricardo Pérez-
6 Enríquez and Janeth Valadez-Rodríguez who provided microsattelites of *L.*
7 *guttatus*. José Francisco Domínguez-Contreras provided technical support in the
8 laboratory. We also thank Diana Cecilia Escobedo Urías from CIDIIR-Guasave for
9 providing housing and transportation during our stay in Sinaloa, Vicente Hernández
10 C. (CRIP Mazatlán) and the fishermen of cooperative “Horacio Fierro” at Huitusi
11 and “San Carlos” at Topolobampo for providing support during sampling. Also, we
12 thank Kristen Gruenthal who provided editing services.

13 **Introduction**

14 One of the strongest drivers of genetic structure within a species is
15 connectivity, the demographic linking of local populations via larval dispersal or
16 movement of juveniles or adults. For instance, connectivity influences almost all
17 ecological and evolutionary processes in metapopulations (Beldade et al. 2014). In
18 a metapopulation, subpopulations are linked through dispersal as sources or sinks
19 at one or more points during the species’ life cycle (Kritzer and Sale 2006). An
20 understanding of spatial and temporal connectivity is therefore an essential
21 prerequisite for devising effective fishery management and conservation strategies
22 under a metapopulation perspective (Fogarty and Botsford 2007, Munguia-Vega et
23 al. 2014).

1 Inferring a metapopulation structure in marine fishes from genetic data can
2 be challenging, however, due to the presence of very low levels of genetic
3 differentiation (e.g. as measured by F_{ST} values) (Hedgecock et al. 2007; Crandall
4 et al. 2018). Such species often have a planktonic larval stage and large population
5 sizes, and it is thus commonly difficult to differentiate between a model of
6 panmixia, where mating is random and demographic rates are homogeneous, and
7 a metapopulation model, with variable movement and demographics among sites
8 (Waples 1998). Nevertheless, each of these two scenarios have important but
9 distinct implications for the sustainable management of fishery resources (MSC
10 2014; Goethel and Berger 2017).

11 Recently, the understanding of metapopulation dynamics has been
12 improved by multidisciplinary approaches in which oceanographic modelling
13 provides information regarding the direction and magnitude of water currents on
14 the dispersal of eggs and larvae of marine species (Soria et al. 2012, Lodeiros et
15 al. 2016) and genetic studies measure gene flow among locations, aiding the
16 validation of the oceanographic modelling (Soria et al. 2012, Munguia-Vega et al.
17 2014, Pascual et al. 2017).

18 The Gulf of California (GC) in Mexico is a semi-enclosed sea with intense
19 currents. GC surface circulation is characterized by a strong mesoscale
20 component, including fronts and eddies, related to the seasonality of the currents
21 and their interaction with the bathymetry (Lavín et al. 2013, Lavín et al. 2014). The
22 Southern Gulf of California (SGC) is an area of the GC where eddies ~70-120 km
23 in diameter are common, connecting both the peninsular (Baja California) and

1 mainland coasts on either side of the SGC (Pegau et al. 2002, Marinone 2012,
2 Sánchez-Velasco et al. 2013, Zavala-Sansón 2015).

3 Modelling studies of larval dispersal in the SGC generally hypothesize
4 higher larval retention along the peninsular coast, where the currents may flow
5 opposite directions at varying depths, resulting in weak coastal currents overall and
6 the trapping of larvae in eddies. In contrast, larval dispersal along the mainland
7 coast appears driven by strong, largely unidirectional coastal currents (Marinone
8 2012, Santiago-García et al. 2014).

9 Some studies of larval fish assemblages in the GC have suggested that
10 these peninsular eddies could transport fish larvae between the peninsular and
11 mainland coasts, although this assumption has not been empirically proven
12 (Hammann et al. 1998, Contreras-Catala et al. 2012, Sánchez-Velasco et al.
13 2013). Thus, it is not yet clear how the hydrodynamics of the SGC can influence
14 larval transport of commercially important fish species across the Gulf.

15 *Lutjanus argentiventris* is a coastal-demersal fish which is distributed from
16 California, USA, to Peru, including both coasts of the GC (Fischer et al. 1995). This
17 species is considered an important resource for small-scale fisheries in the SGC
18 (Aburto-Oropeza et al. 2009). However, a reported catch volume of 252 tons in the
19 peninsular coast of the SGC in 2010 decreased to 103 tons in 2014 (Plomozo-
20 Lugo et al. 2018). The species shows ontogenetic habitat shifts during its life cycle;
21 adults form spawning aggregations near the continental shelf from May to
22 September (Aburto-Oropeza et al. 2009, Erisman et al. 2010, Piñón et al. 2009),
23 although spawning has also been reported during winter in the eastern SGC

1 (Sinaloa) (Piñón et al. 2009). Larval dispersal is driven by oceanographic
2 circulation, followed by recruitment of juveniles (Claro and Lindeman 2008) to
3 mangroves in nearby (retention) or distant sites (export) after 20-26 days of larval
4 development (Zapata and Herrón 2002, Aburto-Oropeza et al. 2009). Adults are
5 found on shallow rocky reefs (20 m) and seamounts (30 m), and moderate fidelity
6 to their home reef has been reported, with movements on the scale of ~3 km
7 (Tinhan et al. 2014, Green et al. 2015). *L. argentiventris* habitat is not distributed
8 homogeneously in the SGC, and the species is likely to survive only within networks
9 of patches that are sufficiently connected by larval dispersal (Kindlmann and Burel
10 2008) or adult migration (Beldade et al. 2014).

11 Given the intense mesoscale activity in the SGC, with summer eddies and
12 currents as potential mechanisms for dispersal of fish larvae, patchy distribution of
13 habitat, and presence of a summer reproductive season, we hypothesized that *L.*
14 *argentiventris* in the SGC could exhibit a metapopulation structure. Given our
15 hypothesis of metapopulation dynamics, we used a multidisciplinary approach that
16 employed both population genetic analyses and mathematical modelling of
17 currents to evaluate connectivity and larval transport routes among *L.*
18 *argentiventris* populations in the SGC.

19 **Materials and methods**

20 *Sampling*

21 Fin clips (caudal or pectoral) of *Lutjanus argentiventris* were obtained from
22 adults and juveniles collected near rocky reefs and mangroves, respectively. Six

1 sites on the peninsular side San Jose (SJ), Francisquito (F), Espiritu Santo (ES),
2 Gaviota (G), Cetmar (C), Mogote (M) and three sites on the mainland side
3 Topolobampo (T), Huitusi (H) and Altata (A) were sampled in the SGC during May
4 2015 through August 2016 (Fig. 1). Immediately after their collection, the samples
5 were preserved in 80% ethanol. The empirically-determined length at sexual
6 maturity was used to discern between adults (≥ 32 cm) and juveniles (< 32 cm)
7 (Piñón et al. 2009). Out of 233 collected specimens, 30 were adults and 203 were
8 juveniles (Table 1).

9 *Development of microsatellites*

10 Novel microsatellite loci for *L. argentiventris* were isolated from an enriched
11 genomic library following the method proposed by Glenn and Schable (2005).
12 Forty-six sequences were of good quality and 30 were useful for primer design
13 using PRIMER3 (Untergasser et al. 2012).

14 Genomic DNA from *L. argentiventris* was extracted from fin clips of 32
15 individuals collected at Espiritu Santo (ES), Baja California Sur, Mexico, using the
16 modified salt extraction method of Lopera-Barrero et al. (2008). Fifty-two
17 microsatellites were tested in the ES sample: 30 isolated de novo in *L.*
18 *argentiventris* (described above), 16 microsatellites isolated from the congener *L.*
19 *peru* (Paz-García et al. 2016), and six microsatellites from *L. guttatus* (Valadez-
20 Rodríguez 2017). Polymerase chain reaction (PCR) amplifications were conducted
21 in a volume of 15 μ L, with 2 μ L of DNA (100 ng μ L⁻¹), 1X PCR buffer, 0.2 mM each
22 dNTP, 2.1 mM MgCl₂, 0.3 U of Taq platinum (Invitrogen), 0.2 μ M of fluorescently-
23 labeled M13 primer (FAM, PET, VIC, NED), 0.033 μ M of forward primer containing

1 an M13 sequence tag in the 5' end (5' TGT AAA ACG ACG GCC AGT 3')
2 (Schuelke 2000), and 0.33 μ M of reverse primer. A touchdown PCR was used in a
3 thermal-cycler (Bibby Scientific Ltd, Staffordshire, UK): 94°C for 5 min; 15 cycles of
4 94°C for 30 s, 65-50°C for 30 s (decreasing 1°C every cycle), 72°C for 30 s; 40
5 cycles of 94 °C for 30 s, 55°C for 30 s and 72°C for 30 s; and a final extension of
6 72°C for 5 min (Munguía-Vega et al. 2013). PCR products were verified in 1.5%
7 agarose gels stained with 8.6X GelRed (Biotium). PCR products of the expected
8 size were sent for fragment analysis on an automated sequencer (ABI3730XL,
9 Applied Biosystems, Carlsbad, CA.) at the University of Arizona Genetics Core in
10 Tucson, AZ, USA.

11 *Population genetic analysis*

12 Genomic DNA extracts (N = 201) from all remaining study locations were
13 obtained with the salt extraction method. All DNA were standardized at 100 ng μ L⁻¹
14 before PCR. Amplifications and fragment analyses were carried out as described
15 previously. Twelve microsatellite loci (Larg1, Larg4, Larg5, Larg11, Larg19, Larg27,
16 Lupe1, Lupe29, Lupe34, Lupe39, Lupe62 and Lgut19) (Table S1) were used in
17 population genetic analyses.

18 Microsatellite genotyping of individuals was performed with the GeneMarker
19 software (SoftGenetics) and classified into bins with FLEXIBIN (Amos et al. 2007).
20 The number of alleles per locus (N_a), effective number of alleles (N_e) and
21 observed (H_o) and expected (H_e) heterozygosities were estimated with GenAlex
22 (Peakall and Smouse 2012). The Hardy-Weinberg equilibrium (HWE) was
23 evaluated in Genepop (Raymond and Rousset 1995) and linkage disequilibrium

1 (LD) between every pair of loci was tested in Fstat (Goudet 1995). The levels of
2 significance of multiple tests in HWE and LD were adjusted ($\alpha = 0.05$) with the
3 Bonferroni approach (Rice 1989). Null allele frequencies (Brookfield method),
4 scoring errors due to stuttering, and evidence of large allelic dropout were
5 estimated using Micro-checker (Van Oosterhout et al. 2004). Allelic distribution was
6 assessed between all pairs of locations (Fisher exact test). Normality (Kolmogorov-
7 Smirnov), homoscedasticity (Levene's) and ANOVA for some genetic diversity
8 indexes (N_e , H_o) were tested.

9 The genetic relatedness between pairs of individuals, a proxy for levels of
10 local larval retention within each location (Cisneros-Mata et al. 2018) was
11 calculated with the estimator of Queller and Goodnight (1989). The mean and the
12 statistical significance (999 permutations, 1000 bootstraps) for each location were
13 obtained with the software GENALEX (Peakall and Smouse 2012).

14 The possible effect of the presence of null alleles in the population genetic
15 structure was evaluated with the following criteria: If the mean frequency of null
16 alleles per locus was equal to or greater than 0.05 and the population deviated
17 from HWE after sequential Bonferroni correction, this locus was candidate for
18 discard from the data. Further, to evaluate whether a candidate locus had a
19 significant effect on the F_{ST} , analyses with and without these microsatellite loci
20 were carried out in ARLEQUIN ver. 3.5.1.2. (Excoffier et al. 2005).

21 Genetic differentiation among sites was assessed with F_{ST} (Weir and
22 Cockerham 1984), paired F_{ST} , a global analysis of molecular variance (AMOVA),
23 and a hierarchical AMOVA between the peninsular and mainland sites. Global and

1 hierarchical AMOVAs (10,000 permutations each) were carried out with the
2 software ARLEQUIN ver. 3.5.1.2. (Excoffier et al. 2005).

3 We implemented three independent runs for a Bayesian clustering analysis
4 with the software STRUCTURE, with the following conditions: admixture model,
5 correlated allele frequencies, 10 Ks, and 10 runs of 1,000,000 Markov chain Monte
6 Carlo iterations per K from which the first 25% were discarded as burn-in. The ΔK
7 and the average of membership coefficient (Q) were calculated (Hubisz et al.
8 2009).

9 The statistical power of the 12 microsatellite loci used to detect genetic
10 differentiation was obtained with the software POWSIM (Ryman and Palm 2006)
11 through Fisher-exact and Chi-square tests (10,000 dememorizations, 1000
12 batches, 10,000 iterations per batch) on samples of 24 individuals. After that 500
13 replicates of populations diverged to a predefined F_{ST} of 0.001 and 0.0025 from a
14 common population with an effective population size of 2000, after 10 generations
15 in drift.

16 To calculate the number of migrants (Nm), an estimator of the gene flow
17 between pairs of locations, the private alleles method was used, where
18 $e^{((\ln(pl)+2.44)/-0.505)}$ (Slatkin 1985) and pl was the mean frequency of private alleles.

19 To assess if *L. argentiventris* populations showed an isolation by distance, a
20 correlation between the geographic and genetic distances was carried out by a
21 Mantel test with 10,000 permutations using GENETIX software.

22 *Oceanographic model*

1 The Regional Oceanic Model System (ROMS) is a high-resolution ocean
2 model that helps to solve the ocean movement at different scales, with a good
3 approximation of the behaviour of the ocean. It works with initial and frontier
4 conditions from observed data on temperature, wind, sea level, currents, tides and
5 other global models (Haidvogel et al. 2000).

6 The ROMS was applied using one layer (mixed layer, 50m deep
7 approximately), a resolution of 3 km, and a monthly climatology of currents (June-
8 August) at the peak of the reproductive season of *L. argentiventris* from 1980
9 through 2005. Larval transport, assumed as the transport of inert particles, was
10 assessed in 22 areas through a period of 20 days of drift (Fig. 1). These areas
11 were defined as the possible sites of spawning of *L. argentiventris*, and the 20 days
12 of drift was approximated the time of larval development in lutjanids from egg to
13 flexion stage (Emata et al. 1994, Drass et al. 2000, Abdo de la Parra et al. 2015).
14 In general, three main steps were involved to run the ROMS: 1) obtaining the
15 currents of the model from the implementation of the ROMS to the Gulf of
16 California; 2) releasing inert particles throughout the Gulf of California domain and
17 applying a lagrangian particle tracking model, and 3) implementing a Markovian
18 algorithm to quantify and synthesize lagrangian trajectory information in terms of
19 probability (Parés-Sierra et al. 2018). The time of arrival and the probability was
20 divided to obtain the most probable days of arrival. Connectivity matrices for each
21 month of study were then calculated with the software Ferret
22 (<http://ferret.pmel.noaa.gov/Ferret/documentation/users-guide>) using the minimum
23 value of the probability of arrival in each of the 22 areas.

1 *Genetic and modelled connectivity network*

2 First generation migrants (fgm) were detected using a Bayesian approach
3 for assignment with the software GENECLASS2 (Piry et al. 2004). We simulated
4 100,000 individuals employing the resampling algorithm of Rannala and Mountain
5 (1997), which is a statistical method used to identify individuals who are immigrants
6 or have recent immigrant ancestry and is appropriate for use with microsatellite
7 markers. An alpha value of 0.001 and the statistical index $fgm = L_{home}/L_{max}$
8 (Peatkau et al. 2004) were used. Here, L_{home} is the likelihood that an individual
9 genotype belongs to the population from which it was sampled, given the observed
10 allele frequencies, and L_{max} is the maximum likelihood observed for this genotype
11 in any population (Peatkau et al. 2004). We identified individual migrants as those
12 showing $\geq 99\%$ threshold probability value.

13 We used a graph-theoretic approach (Trembl et al. 2008, Munguia-Vega et al.
14 2014) to construct a spatial network of nodes (sites) connected by links
15 represented either by the genetic (fgm) or the oceanographic modelling data (larval
16 dispersal). Marine connectivity patterns were displayed as spatial graphs with the
17 tool XY to line in the software ArcMap 10. For the genetic data, we used the source
18 and target geographic coordinates based on fgm results and the frequency of each
19 connection. For the modelled data, we used the source and target geographic
20 coordinates, based on tracking particle trajectories, and the probability of each
21 connection between locations. Given the resolution of our oceanographic model,
22 genetic samples from San Jose (SJ) and Francisquito (F), Espiritu Santo (ES) and
23 Gaviota (G), and Cetmar (C) and Mogote (M), respectively, were analysed jointly

1 within the same spatial unit of the modelled data in order to make comparisons of
2 both connectivity networks. In-degree (number of connections that enter a site) and
3 out-degree (number of connections leaving a site) at each location were estimated
4 for the genetic and modelled data with the software GEPHI (Bastian et al. 2009).

5 *Gene-flow models*

6 In order to test a recent approach based on the coalescent, which considers
7 demography and metapopulation history separately, MIGRATE-n was implemented
8 (Beerli and Palczewski 2010). Five different population genetic scenarios regarding
9 the directionality of average gene flow patterns among the localities were tested: 1)
10 one model with one population size, where all localities were part of the same
11 panmictic population; 2) one full migration model with six population sizes [San
12 Jose-Francisquito (SJ-F), Espiritu Santo-Gaviota (ES-G), Cetmar-Mogote (C-M),
13 Topolobampo (T), Huitusi (H) and Altata (A)] and 36 directional migration rates
14 among all possible pairs of sites; and 3) three models with asymmetric connections
15 among sites during June, July and August, as suggested by the ROMS
16 oceanographic model, using six population sizes and 17, 9 and 11 directional
17 migration rates, respectively. Three independent runs were performed for each
18 model, with a Bayesian inference approach; a Brownian motion mutation model; a
19 constant mutation rate for all loci was assumed; the proposal distribution for Θ and
20 M was metropolis sampling, where Θ is the mutation-scaled effective population
21 size for the recipient populations and M is the mutation-scaled migration rate
22 (Beerli 2009); the start values for Θ and M were generated from F_{ST} calculations;
23 the prior distribution of the parameters for Θ was a minimum of 0.0, maximum 0.1

1 and delta 0.01 and for M was a minimum of 0.0, maximum 1000 and delta 100;
2 100,000 recorded steps from which the first 25% were discarded as burn-in; one
3 long chain and four heated chains under a static heating scheme (uniform priors);
4 and a swapping interval of 10. To test if results were affected by the use of narrow
5 priors for Θ and M, we conducted a set of identical runs of the five scenarios with
6 the following prior distribution parameters: a minimum of 0, maximum of 0.4 and
7 delta of 0.04 for Θ and a minimum of 0, maximum of 1000 and a delta of 100 for M.

8 The ratio of the marginal likelihood was used to select the best model
9 supported by the genetic data as indicated by the highest natural log Bayes factor
10 with the Bezier approximation (Beerli and Palczewski 2010). The number of
11 migrants per generation was calculated as follows: $Nm = \theta * (M/4)$. To estimate
12 the role of each population as source or sink, we subtracted the total Nm leaving
13 from the Nm entering each site (Munguia-Vega et al. 2018).

14 **Results**

15 *Characterization of microsatellites*

16 Of the 52 microsatellites tested, 18 were successfully genotyped. Significant
17 deviations from Hardy-Weinberg equilibrium ($p < 0.004$) were observed in five loci
18 after the Bonferroni test due to a deficit of heterozygotes and presence of null
19 alleles. Thus, thirteen microsatellite loci were candidates for the population genetic
20 analyses. We then excluded one additional locus not in HWE (Lupe55 $p = 0.026$)
21 (Table S1). Nine loci presented 4-14 alleles, and three loci 17-24 alleles. The
22 probability of identity with 12 microsatellite loci was 7.9×10^{-14} , meaning that 1 in

1 about 12.6 billion individuals would have exactly the same multilocus genotype by
2 chance.

3 *Genetic diversity*

4 After the sequential Bonferroni adjustment, no LD ($p < 0.0007$) was
5 observed from a total of 108 pairwise comparisons, and only four tests (3.7%)
6 showed significant deviations ($p < 0.0005$) from HWE. Such deviations were due to
7 heterozygote deficits and the presence of null alleles at low or moderate
8 frequencies, ranging from 0.097 to 0.193 (Table S2), in a few sites.

9 We found moderate levels and little variation in genetic diversity in *L.*
10 *argentiventris* among localities. Mean N_a ranged from 6.58 - 10.75; mean N_e
11 ranged from 4.64 - 6.19, and mean H_o and H_e ranged from 0.63 - 0.70. Mean
12 private alleles were present in all the localities, except in San Jose (SJ), and
13 ranged from 0.25 – 1.4 alleles per locus. Cetmar (C) showed the highest number of
14 alleles, effective number of alleles and number of private alleles but presented one
15 of the lowest observed heterozygosities, due to a deficit of heterozygotes, while
16 Topolobampo (T) showed the lowest number of alleles and effective number of
17 alleles but one of the highest observed heterozygosities. Finally, Espiritu Santo
18 (ES) showed the highest observed heterozygosity (Fig. 2). However, allelic
19 distributions among locations were not significantly different from each other after
20 sequential Bonferroni adjustment ($p > 0.009$), and N_e and H_o showed no
21 significant differences among locations after ANOVA ($N_e p > 0.83$; $H_o p > 0.45$).

1 Locations showed mean relatedness coefficients (r) ranging from - 0.05 to
2 0.05. Significantly high and low values indicated that individuals sampled were
3 more or less similar to one another, respectively, than would be expected under
4 random mating (Fig. 3). Locations with the highest relatedness coefficients were
5 San Jose (SJ) ($r = 0.048$, $p = 0.05$) and Mogote ($r = 0.031$, $p = 0.8$). In contrast,
6 Espiritu Santo (ES) and Francisquito (F) showed lower relatedness coefficients of -
7 0.05 ($p = 0.008$) and -0.02 ($p = 0.1$), respectively.

8 *Population genetic structure*

9 Global F_{ST} values with ($F_{ST} = -0.00071$, $p = 1$) or without the three loci
10 deviating from HWE and exhibiting high null allele frequencies (Lupe39, Lupe62,
11 and Larg27; $F_{ST} = -0.00089$, $p = 1$) indicated a lack of significant population
12 structure among locations in the SGC. Since the effect of these loci was not
13 significant, all 12 loci were used in subsequent analyses. The statistical power was
14 30% and 80% to detect significant genetic differentiation among populations,
15 based on the level of polymorphism observed among the 12 microsatellite loci, for
16 a predefined $F_{ST} = 0.001$ and 0.0025, respectively.

17 The pairwise F_{ST} values among locations (Table 2) ranged from -0.0086 to
18 0.0158 and were not statistically significant ($p > 0.06$). The hierarchical AMOVA
19 between locations on the peninsular and mainland sides also did not show
20 significant differences ($F_{ST} = 0.001$, $p = 0.66$). Although the ΔK criteria in the
21 Structure analysis suggested the presence of 3 to 4 clusters, the probability of
22 assignment to each cluster was symmetric and all individuals were equally
23 admixed, further indicating a lack of population structure (S3). The number of

1 migrants estimated based on private alleles indicated lower values in Mogote (M)
2 and Topolobampo (T) and higher values in Espiritu Santo (ES), Francisquito (F),
3 and Huitusi (H). The Mantel test did not show a significant relationship between
4 geographic and genetic distances ($r^2 = 0.06$, $p = 0.12$).

5 *Oceanographic model*

6 In general, a pattern of cyclonic circulation was observed in the SGC from
7 June to August. In June, an anticyclonic eddy was found to influence both the
8 peninsular and mainland sides, with velocities of $\sim 0.2 \text{ m s}^{-1}$, and a stream flow
9 (between quadrants 8 and 16) that crosses from the peninsular to mainland sides
10 with velocities of $\sim 0.1 \text{ m s}^{-1}$ (Fig. 4a). The connectivity matrix indicated likely routes
11 of larval transport, with high arrival probability, from the peninsula to the mainland
12 (quadrants 1-5 to 10-14) taking place under a maximum period of 20 days (Fig.
13 4b). Due to the stream flow, additional potential connections from the peninsula to
14 the mainland (quadrants 6-9 to 15-17) were also observed (Fig. 4b). Otherwise, a
15 higher number of south to north connections were observed along the peninsular
16 and mainland sides (Fig. 4b).

17 In July, the model suggested that the anticyclonic eddy dispersed, leaving a
18 stream flow located between quadrants 1 to 10, with velocities of $\sim 0.2 \text{ m s}^{-1}$ (Fig.
19 4c). The connectivity matrix showed connections from the northern part of the
20 peninsula to the mainland (from quadrants 1-4 to 10-15) occurring in a maximum
21 period of 18 days due to the influence of this stream flow (Fig. 4d). Concurrently,
22 an early cyclonic eddy was observed below the stream flow (Fig. 4c), but it did not
23 show connections between the peninsula and mainland. As in June, a higher

1 number of connections along the mainland side were found from southern to
2 northern quadrants due to the persistence of the strong mainland northward
3 current. On the peninsular side, however, such connections were reduced relative
4 to those found in June (Fig. 4d).

5 In August, the stream flow narrowed because of the formation of two
6 cyclonic eddies ($\sim 0.15 \text{ m s}^{-1}$) to the north and south of the stream flow (Fig. 4e).
7 Connections due to this flow remained in the matrix, specifically from the northern
8 part of the peninsula to the mainland (from quadrants 1-4 to 10-14) in a maximum
9 period of 20 days (Fig. 4f). Below the stream flow, the larger and more well-defined
10 cyclonic eddy contributed to a lesser extent with some connections from the central
11 mainland region to the peninsular side (quadrants 15-18 to 4).

12 *Genetic and modelled larval dispersal connectivity networks*

13 The analysis of first generation migrants classified 70 out of 214 individuals
14 (32.7%) as migrants ($p < 0.001$). The genetic connectivity network (Fig. 5) showed
15 a higher frequency of connections from the peninsular coast to the mainland than
16 vice versa, including from San Jose - Francisquito (SJ-F) to Topolobampo (T),
17 Espiritu Santo -Gaviota (ES-G) to Altata (A), and Mogote-Cetmar (M-C) to Altata
18 (A). Further, some connections to the north and south along both coasts were
19 observed, and the majority of them were bidirectional (Fig. 5). In general, the in-
20 degree and out-degree of every sampled location were similar. The locations with
21 the highest in-degree were Espiritu Santo–Gaviota (ES-G) and Mogote-Cetmar (M-
22 C), each with five inbound connections. The locations with the highest out-degree
23 were San Jose-Francisquito (SJ-F), Mogote-Cetmar (M-C), Huitusi (H) and Altata

1 (A), each with five outbound connections (Table 4). The mean number of regional
2 in-degree for the peninsula and mainland were also similar at 4.6 and 4.0,
3 respectively, while the mean number of out-degree was 4.3 for both cases.

4 In general, the modelled connectivity networks indicated transport along the
5 mainland and peninsular sides, mostly from the south towards the north. Transport
6 from the peninsula towards the mainland took place in the northernmost part of the
7 SGC (Fig. 6), where eddies and the stream flow were present. During June and
8 July, in a window of time between 15 to 20 days (during which the larvae of *L.*
9 *argentiventris* may begin to settle), more connections were observed from the
10 peninsular to the mainland side due to the stream flow. Such connections showed
11 probabilities from 0.2-0.6 (Fig. 6a and 6b). In August, more connections were
12 observed between both coasts and in both directions, with probabilities ranging
13 between 0.2-0.4 (Fig. 6c) due to the stream flow couple with a well-defined cyclonic
14 eddy influence. The location with the highest in-degree was Topolobampo (T) on
15 the mainland side with eight inbound connections, and the locations with the
16 highest out-degree was San Jose - Francisquito (SJ-F) in the peninsular side with
17 six outbound connections (Table 5).

18 *Gene-flow models*

19 The Bezier approximation for the three independent runs within each model,
20 showed consistent results, indicating convergence of the MCMC chains (S4). Both
21 sets of Migrate runs with narrow and wide priors produced exactly the same
22 ranking of the five models (Table 6), suggesting the influence of the priors was
23 negligible compared to the information contained in the dataset (Beerli et al. 2019).

1 According to the Bayes factor, the full migration model (model 2, which represents
2 a metapopulation structure, with reciprocal connections of varying intensities
3 among all pairs of sites) was the best-supported model for explaining the observed
4 genetic data. Model 2 was followed in order of best fit by models 3, 5 and 4,
5 representing the oceanographic models from June, August and July, respectively
6 (Table 6). The panmictic model (model 1) was the least supported by the data.
7 Results indicated that the net sources of migrants were located on the peninsular
8 side, while sites located on the mainland side acted as net sinks (Table 7; see
9 Table S5 for details). The most important source of larvae was Espiritu Santo-
10 Gaviota (ES-G) and the most important sink was Huitusi (H).

11 **Discussion**

12 Traditional F_{ST} and hierarchical AMOVA analyses as well as the
13 STRUCTURE clustering analysis did not detect significant differences among
14 studied locations for *Lutjanus argentiventris* from the SGC. The estimations of the
15 number of migrants indicated moderate to high gene flow among locations.
16 However, a coalescent sampler (MIGRATE-n), the analysis of first-generation
17 migrants and the oceanographic simulations suggested the presence of
18 metapopulation structure and asymmetrical gene flow. Although these results could
19 be seen as contradictory, it is possible to reconcile them considering the
20 assumptions of the different analyses and the characteristics of marine
21 populations.

22 Non-significant F_{ST} and hierarchical AMOVA are commonly interpreted as
23 evidence for the presence of a single panmictic population, but is important to

1 highlight that these techniques that rely on the variance in allele frequencies
2 among populations are unable to distinguish between moderate gene flow and
3 random mating, reflect long-term dispersal rates and not respond to real time
4 movement of individuals (Paetkau 2004; Hedgecock et al. 2007; Crandall et al.
5 2018). Both F_{ST} (and AMOVA) show a nonlinear relationship with gene flow such
6 that F_{ST} changes drastically at low levels of gene flow (e.g. $Nm \leq 5$ migrants per
7 generation) but is unable to distinguish among many scenarios where $Nm \geq 10$
8 migrants per generation (Hedgecock et al. 2007). Some recent studies have
9 highlighted that the presence of low F_{ST} values and a metapopulation structure with
10 moderate levels of migration that deviates from panmixia are not mutually
11 exclusive scenarios in marine populations, either. For example, non-significant F_{ST}
12 values have been reported in the presence of metapopulation structure in the form
13 of a stepping-stone model (Crandall et al. 2018) or predominantly asymmetric
14 gene flow among sites exhibiting source-sink dynamics (Cisneros-Mata et al.
15 2018).

16 In contrast, coalescent samplers estimate effective population size and
17 directional migration rates separately, in addition to using information on the
18 genealogy of the samples along with allele frequency data (Beerli et al. 2019).
19 Thus, are able to estimate migration rates at the high levels of gene flow where F-
20 statistics are not useful or have low power (Selkoe et al. 2016, Crandall et al.
21 2018). They also provide appropriate estimates of uncertainty and allow estimation
22 of marginal likelihoods to compare different metapopulation models within the
23 same statistical framework. According to MIGRATE-n, there was a clear

1 geographic clustering of net sources (peninsula) and net sinks of larvae
2 (mainland), a pattern reported previously for at least another fish from the GC
3 (Munguia-Vega et al. 2014).

4 Although MIGRATE-n favoured the presence of metapopulation structure
5 over a panmictic scenario for *L. argentiventris* in the SGC, such interpretation
6 requires some level of skepticism. For example, MIGRATE-n could have difficulties
7 to recover the true model when both N_e and N_m are very large (e.g. $Nem > 1000$)
8 (Crandall et al. 2018). In cases of low genetic differentiation (e.g. $F_{ST} < 0.01$)
9 caution should be taken to avoid statistical artifacts and random genetic patchiness
10 that could provide a false impression of population structure in the absence of it
11 (Hauser and Carvalho 2008). Additionally, individual Bayesian assignment
12 methods as STRUCTURE and the first-generation migrant analysis we
13 implemented in GENECLASS2 are known to perform correct assignments only
14 under conditions of moderate to low gene flow (e.g. $Nm < 5$) (Waples and Gaggiotti
15 2006). Since our results are based on a set of relatively low number of markers
16 showing moderate levels of polymorphism, future studies using more loci
17 throughout the genome (e.g. SNPs) could help to improve the statistical power of
18 analyses to verify levels of metapopulation structure that deviate from panmixia
19 (Bernatchez et al. 2017; Ovenden et al. 2015).

20 We found additional evidence that could be in agreement with the presence
21 of a metapopulation structure, where sites might be acting as sinks or sources of
22 larvae with varying levels of larval export (Waples and Gaggiotti 2006; Ciannelli et
23 al. 2013). The oceanographic ROMS modelling suggested asymmetric currents in

1 the SGC during the spawning period of *L. argentiventris* that resulted in different
2 levels of exchange of migrants between the peninsula and the mainland driven by
3 local eddies and stream flows. The sites analysed behaved like a patchily-
4 distributed population interconnected by dispersal at different rates and directions.
5 Additionally, at least one index of genetic diversity within sites (average
6 relatedness) showed significant variation among locations, suggesting varying
7 levels of local larval retention within sites that also represent a direct evidence of
8 distinct demographic rates at the local level that deviate from panmixia. Other
9 species of fish and invertebrates from the GC show evidence of metapopulation
10 structure driven by strong oceanic currents that mediate larval dispersal, including
11 *Spondylus calcifer* (Soria et al. 2012; Lodeiros et al. 2016) *Mycteroperca rosacea*
12 (Munguia-Vega et al. 2014), *Hyporthodus acanthistius* (Beldade et al. 2014),
13 *Lutjanus peru* (Munguia-Vega et al. 2018b) and *Callinectes bellicosus* (Cisneros-
14 Mata et al. 2018).

15 Our results indicated the existence of mechanisms that enhance the
16 connectivity between the peninsular and mainland coasts. In this respect, two
17 possible mechanisms of connectivity are possible: 1) larval transport by physical
18 factors, such as seasonal currents, eddies, and stream flows that cross the SGC in
19 both directions, and/or 2) juvenile and adult movements during ontogenetic habitat
20 shifts, including spawning migrations (Green et al. 2015). Regarding the first
21 mechanism, studies on the swimming ability of Lutjanidae larvae to overcome the
22 effect of ocean currents support the hypothesis of a nearly passive larval transport.
23 Experiments in laboratory showed that Lutjanidae larvae with sizes smaller than 8

1 mm cannot swim against a current $\geq 0.1 \text{ m s}^{-1}$ (Stobutzki and Bellwood 1997,
2 Fisher et al. 2000, Leis et al. 2007). Studies generating *in situ* physicochemical
3 data in the GC have reported eddies with surface velocities ranging from 0.25 to
4 0.6 m s^{-1} (Contreras-Catala et al. 2012, Sanchez-Velasco et al. 2013, Lavin et al.
5 2014). Hence, it is likely that the early life stages of Lutjanidae cannot evade the
6 currents in the SGC.

7 In terms of the second mechanism, studies in *L. argentiventris* have
8 reported ontogenetic habitat shifts between juveniles that recruit in mangrove
9 habitats at the end of the planktonic larval phase and adults that live on shallow
10 rocky reefs (Aburto-Oropeza et al. 2009). Adult movement reported for lutjanids
11 elsewhere is quite limited, extending $\sim 3 \text{ km}$ from their home rocky reef (Green et
12 al. 2015). In a study of *L. argentiventris* adult movements in the SGC, individuals
13 showed from moderate to high site fidelity during the non-reproductive season.
14 Adults then travelled maximum $\sim 15 \text{ km}$ to reach a spawning aggregation on a
15 nearby seamount (Tinhan et al. 2014). Such behaviour could increase the gene
16 flow between nearby locations. The genetic homogeneity between nearby locations
17 along the same coast is thus probably due, in part, to both mechanisms of
18 connectivity; in addition to larval dispersal, adult migration and ontogenetic habitat
19 shifts over geographic scales of dozens of kilometres does occur and likely follows
20 a stepping-stone model. Meanwhile, although migration of adults across the
21 oceanic basins in the SGC cannot be discounted, genetic homogeneity between
22 both coasts in the SGC probably is enhanced by larval dispersal, driven by

1 mesoscale eddies, stream flows (as the modelled oceanography potentially
2 suggests) and habitat availability for subsequent life stages.

3 *Lutjanus argentiventris* showed lower genetic diversity compared with
4 another Lutjanids from the same study area (*L. peru*, Munguia-Vega et al. 2018b).
5 This variation among the species could be related to differences in effective
6 population size or the polymorphism of the genetic markers. Some of the studied
7 sites, such as Cetmar (C), Francisquito (F) and Espiritu Santo (ES), showed
8 genetic patterns characteristic of population sinks, including a high number of
9 alleles and effective alleles, a deficit of heterozygotes that could be caused by a
10 Wahlund effect or a mixture of different populations (Freeland, 2006), lower
11 relatedness, and a high number of migrants (Nm). These characteristics are
12 expected when a site receives migrants from multiple sources (Munguia-Vega et
13 al. 2018b). It should be noted, however, that while these speculations are in
14 agreement with the genetic network, they do not conform to the modelled
15 oceanographic network. Meanwhile, San Jose (SJ) did not have private alleles,
16 which is a strong indicator of its potential role as larval source, exporting its genetic
17 signature to other sites. This hypothesis was also supported by a high out-degree
18 in both genetic and modelled networks. This site also showed higher relatedness,
19 indicating there may be some local retention of larvae (Teske et al. 2016), although
20 this was not predicted by the oceanographic model.

21 The mismatch between the genetic data and the ocean models regarding
22 the source-sink role of some sites along the peninsular coast could be explained by
23 several factors: 1) winter circulation was not modelled, although Piñon et al. (2009)

1 suggested a spawning period during winter for *L. argentiventris* at mainland sites;
2 2) the scale of the ocean model was much larger than the scale of genetic
3 sampling, and in some cases, multiple genetic sites were included within a single
4 spatial unit used for the ocean model; 3) a monthly climatology was used in the
5 model and the variability of the eddies was likely underestimated; 4) the model did
6 not incorporate larval behaviour; 5) some potential spawning sites were likely not
7 included in our simulations; 6) larval dispersal could be effectively different from
8 gene flow because the latter assumes survival of larvae up to reproduction
9 (Hellberg et al. 2002); and finally, 7) in contrast to the seasonal patterns of larval
10 dispersal during a typical year included in the model, the genetic data reflects an
11 average across multiple generations, each the product of distinct spawning
12 seasons. At least 16 no-take marine reserves exist along the peninsular coast of
13 the SGC, all aimed at recovering the biomass, species and genetic diversity and
14 individual size, age and reproductive potential of important fishery species
15 (Munguia-Vega et al. 2018a). While our results suggest the location of these
16 reserves is correct, given the role of peninsular populations as sources of
17 individuals in the SGC, protecting nursery areas (mangroves) is also key to
18 maintaining a viable metapopulation structure as well as supporting important
19 small-scale fisheries in the region.

20 **Compliance with ethical standards**

21 *Founding:* This research was supported by CONACyT grants (CB2015-
22 257019) from Noé Díaz-Viloria and (CB2014-236864-T) from Laura Sánchez-
23 Velasco, IPN-SIP (20160514, 20170290, 20180339, 20195461) grants to Noé

1 Díaz-Viloria, and The David and Lucile Packard Foundation grants to the PANGAS
2 Science Coordination. Nicole Reguera-Rouzaud was a recipient of a BEIFI-IPN
3 and a CONACYT scholarship (No. 589502).

4 *Conflict of interest:* the authors declare that they have no conflict of interest.

5 *Ethical approval:* All applicable international, national, and/or institutional guidelines
6 for the care and use of animals were followed.

7 *Sampling and field studies:* The samples were obtained from the fishing
8 cooperatives of the region. All necessary permits for sampling were obtained
9 (PPF/DGOPA-057/18).

10 *Data availability:* The datasets generated during and/or analysed during the current
11 study are available from the corresponding author on reasonable request. The
12 most relevant information are in supplementary information file. We generated all
13 the data during this research. We do not used public data.

14 **Literature cited**

15 Abdo de la Parra MI, Rodríguez-Ibarra LE, Rodríguez Montes de Oca G, et al
16 (2015) Estado actual del cultivo de larvas del pargo flamenco (*Lutjanus*
17 *guttatus*). Lat Amercian J Aquat Res 43:415–423.

18 Aburto-Oropeza O, Dominguez-Guerrero I, Cota-Nieto J, Plomozo-Lugo T (2009)
19 Recruitment and ontogenetic habitat shifts of the yellow snapper (*Lutjanus*
20 *argentiventris*) in the Gulf of California. Mar Biol 156:2461–2472.

21 Amos W, Hoffman JI, Frodsham A, et al (2007) Automated binning of microsatellite

1 alleles: Problems and solutions. *Mol Ecol Notes* 7:10–14.

2 Bastian M, Heymann S, Jacomy M (2009) Gephi: An open source software for
3 exploring and manipulating networks. In: International AAAI conference on
4 weblogs and social media. AAAI Press, San Jose, California

5 Beerli P (2009) How to use MIGRATE or why are Markov chain Monte Carlo
6 programs difficult to use? In: *Populations Genetics for Animal Conservation*. p
7 395

8 Beerli P. Mashayekhi S. Sadeghi M. Khodaei M. Shaw K. (2019) Population
9 genetic inference with MIGRATE. *Current Protocols in Bioinformatics*, 68, e87.
10 doi: 10.1002/cpbi.87.

11 Beerli P, Palczewski M (2010) Unified framework to evaluate panmixia and
12 migration direction among multiple sampling locations. *Genetics* 185:313–326.

13 Beldade R, Jackson AM, Cudney-Bueno R, et al (2014) Genetic structure among
14 spawning aggregations of the gulf coney *Hyporthodus acanthistius*. *Mar Ecol*
15 *Prog Ser* 499:193–201.

16 Bernatchez, L., Wellenreuther, M., Araneda, C., Ashton, D. T., Barth, J. M. I.,
17 Beacham, T. D., Maes, G. E., et al. 2017. Harnessing the power of genomics
18 to secure the future of seafood. *Trends in Ecology & Evolution*, 32: 665-680.

19 Ciannelli L, Fisher JAD, Skern-Mauritzen M, et al (2013) Theory, consequences
20 and evidence of eroding population spatial structure in harvested marine
21 fishes: A review. *Mar Ecol Prog Ser* 480:227–243.

- 1 Cisneros-Mata MA, Munguía-Vega A, Rodríguez-Félix D, et al (2018) Genetic
2 diversity and metapopulation structure of the brown swimming crab
3 (*Callinectes bellicosus*) along the coast of Sonora , Mexico : Implications for
4 fisheries management. Fish Res 212:97–106.
- 5 Claro R, Lindeman KC (2008) Biología y manejo de los pargos (Lutjanidae) en el
6 Atlántico occidental, Instituto. La Habana, Cuba
- 7 Contreras-Catala F, Sanchez-Velasco L, Lavin MF, Godinez VM (2012) Three-
8 dimensional distribution of larval fish assemblages in an anticyclonic eddy in a
9 semi-enclosed sea (Gulf of California). J Plankton Res 34:548–562.
- 10 Crandall ED, Toonen RJ, Laboratory T, Selkoe KA (2018) A coalescent sampler
11 successfully detects biologically meaningful population structure overlooked by
12 F-statistics. Evol Appl 12:255–265.
- 13 Drass DM, Bootes KL, Lyczkowski-Shultz J, et al (2000) Larval development of red
14 snapper, *Lutjanus campechanus*, and comparisons with co-occurring snapper
15 species. Fish Bull 98:507–527
- 16 Emata AC, Eullaran B, Bagarinao TU, et al (1994) Induced spawning and early life
17 description of the mangrove red snapper, *Lutjanus argentimaculatus*.
18 Aquaculture 121:381–387.
- 19 Erisman B, Mascarenas I, Paredes G, et al (2010) Seasonal, annual, and long-
20 term trends in commercial fisheries for aggregating reef fishes in the Gulf of
21 California, Mexico. Fish Res 106:279–288.
- 22 Excoffier L, Laval G, Schneider S (2005) Arlequin (version 3.0): an integrated

1 software package for population genetics data analysis. *Evol Bioinform Online*
2 1:47–50.

3 Fischer W, Krupp F, Schneider W, et al (1995) Guía FAO para la identificación de
4 especies para los fines de pesca. Pacífico centro-oriental. Volumen III.
5 Vertebrados - Parte 2. Roma

6 Fisher R, Bellwood DR, Job SD (2000) Development of swimming abilities in reef
7 fish larvae. *Mar Ecol Prog Ser* 202:163–173.

8 Fogarty MJ, Botsford LW (2007) Population connectivity and spatial management
9 of marine fisheries. *Oceanography* 20:112–123.

10 Glenn TC, Schable NA (2005) Isolating microsatellite DNA loci. *Methods Enzymol*
11 395:202–222.

12 Goethel DR, Berger AM (2017) Accounting for spatial complexities in the
13 calculation of biological reference points: Effects of misdiagnosing population
14 structure for stock status indicators. *Can J Fish Aquat Sci* 74:1878–1894.

15 Goudet J (1995) FSTAT (Version 1.2): A computer program to calculate F-
16 statistics. *J Hered* 86:485–486.

17 Green AL, Maypa AP, Almany GR, et al (2015) Larval dispersal and movement
18 patterns of coral reef fishes, and implications for marine reserve network
19 design. *Biol Rev* 90:1215–1247.

20 Haidvogel DB, Arango HG, Hedstrom K, et al (2000) Model evaluation experiments
21 in the North Atlantic Basin: Simulations in nonlinear terrain-following

1 coordinates. *Dyn Atmos Ocean* 32:239–281.

2 Hammann MG, Nevárez-Martínez MO, Green-Ruíz Y (1998) Spawning habitat of
3 the Pacific sardine (*Sardinops sagax*) in the Gulf of California: Egg and larval
4 distribution 1956-1957 and 1971-1991. *Calif Coop Ocean Fish Investig Rep*
5 39:169–179

6 Hauser, L., and Carvalho, G. R. 2008. Paradigm shifts in marine fisheries genetics:
7 Ugly hypotheses slain by beautiful facts. *Fish and Fisheries*, 9: 333-362.

8 Hedgecock D, Barger PH, Edmands S (2007) Genetic approaches to measuring
9 connectivity. *Oceanography* 20:70–79

10 Hellberg ME, Burton RS, Neigel JE, Palumbi SR (2002) Genetic assesment of
11 connectivity among marine populations. *Bull Mar Sci* 70:273–290

12 Hubisz MJ, Falush D, Stephens M, Pritchard JK (2009) Inferring weak population
13 structure with the assistance of sample group information. *Mol Ecol Resour*
14 9:1322–1332.

15 Kindlmann P, Burel F (2008) Connectivity measures: A review. *Landsc Ecol*
16 23:879–890.

17 Kritzer JP, Sale PF (2006) The metapopulations Ecology of Coral Reef Fishes. In:
18 *Marine Metapopulations*. pp 31–67

19 Lavín MF, Castro R, Beier E, Godínez VM (2013) Mesoscale eddies in the
20 southern Gulf of California during summer: Characteristics and interaction with
21 the wind stress. *J Geophys Res Ocean* 118:1367–1381.

- 1 Lavín MF, Castro R, Beirer E, et al (2014) Surface circulation in the Gulf of
2 California in summer from surface drifters and satellite images (2004-2006). J
3 Geophys Res Ocean 119:4278–4290
- 4 Leis JM, Hay AC, Lockett MM, et al (2007) Ontogeny of swimming speed in larvae
5 of pelagic-spawning , tropical , marine fishes. Mar Ecol Prog Ser 349:255–267.
- 6 Lodeiros C, Soria G, Valentich-Scott P, et al (2016) Spondylids of Eastern Pacific
7 Ocean. J Shellfish Res 35:279–293.
- 8 Lopera-Barrero NM, Povh J a, Ribeiro RP, et al (2008) Comparación de protocolos
9 de extracción de ADN con muestras de aleta y larva de peces: extracción
10 modificada con cloruro de sodio. Cienc e Investig Agrar 35:77–86.
- 11 Marinone SG (2012) Seasonal surface connectivity in the Gulf of California. Estuar
12 Coast Shelf Sci 100:133–141.
- 13 MSC (2014) Marine Stewardship Council Fisheries Certifications Requirements
14 and Guidance
- 15 Munguia-Vega A, Green AL, Suarez-Castillo AN, et al (2018a) Ecological
16 guidelines for designing networks of marine reserves in the unique biophysical
17 environment of the Gulf of California. 28:749–776.
- 18 Munguia-Vega A, Jackson A, Marinone SG, et al (2014) Asymmetric connectivity of
19 spawning aggregations of a commercially important marine fish using a
20 multidisciplinary approach. PeerJ 2:511.
- 21 Munguía-Vega A, Klimova A, Culver M (2013) New microsatellites loci isolated via

1 next-generation sequencing for two endangered pronghorn from the Sonoran
2 Desert. *Conserv Genet Resour* 53:1689–1699.

3 Munguia-Vega A, Marinone SG, Paz-Garcia DA, et al (2018b) Anisotropic larval
4 connectivity and metapopulation structure driven by directional oceanic
5 currents in a marine fish targeted by small-scale fisheries. *Mar Biol* 165:16.

6 Ovenden, J. R., Berry, O., Welch, D. J., Buckworth, R. C., and Dichmont, C. M.
7 2015. Ocean's eleven: A critical evaluation of the role of population,
8 evolutionary and molecular genetics in the management of wild fisheries. *Fish*
9 *and Fisheries*, 16: 125-159.

10 Paetkau D, Slade R, Burden M, Estoup A (2004) Genetic assignment methods for
11 the direct, real-time estimation of migration rate: a simulation-based
12 exploration of accuracy and power. *Mol Ecol* 13:55–65.

13 Parés-Sierra A, Flores-Morales AL, Gómez-Valdivia F (2018) An efficient
14 Markovian algorithm for the analysis of ocean currents. *Environ Model Softw*
15 103:158–168.

16 Pascual M, Rives B, Schunter C, Macpherson E (2017) Impact of life history traits
17 on gene flow: A multispecies systematic review across oceanographic barriers
18 in the Mediterranean Sea. *PLoS One* 12:1–20.

19 Paz-García DA, Munguía-Vega A, Plomozo-Lugo T, Hudson-Weaver A (2016)
20 Characterization of 32 microsatellite loci for the Pacific red snapper *Lutjanus*
21 *peru* through next generation sequencing. *Mol Biol Rep* 44:251–256

22 Peakall R, Smouse PE (2012) GenALEX 6.5: Genetic analysis in Excel. *Population*

- 1 genetic software for teaching and research-an update. *Bioinformatics*
2 28:2537–2539.
- 3 Pegau WS, Boss E, Martínez A (2002) Ocean color observations of eddies during
4 the summer in the Gulf of California. *Geophys Res Lett* 29:29–31
- 5 Piñón A-, Amezcua F, Duncan N (2009) Reproductive cycle of female yellow
6 snapper *Lutjanus argentiventris* (Pisces, Actinopterygii, Lutjanidae) in the SW
7 Gulf of California: gonadic stages, spawning seasonality and length at sexual
8 maturity. *J Appl Ichthyol* 25:18–25.
- 9 Piry S, Alapetite A, Cornuet JM, et al (2004) GENECLASS2: A software for genetic
10 assignment and first-generation migrant detection. *J Hered* 95:536–539.
- 11 Plomozo-Lugo T, Weaver AH, González-Cuellar OT (2018) Resultados del
12 esfuerzo de monitoreo pesquero y de las bitácoras pesqueras de 2016 y
13 2017. 5to taller de Técnicos Pesqueros. La Paz, B.C.S.
- 14 Queller DC, Goodnight KF (1989) Estimating Relatedness Using Genetic Markers.
15 *Evolution* (N Y) 43:258–275.
- 16 Rannala B, Mountain JL (1997) Detecting immigration by using multilocus
17 genotypes. *Proc Natl Acad Sci U S A* 94:9197–9201.
- 18 Raymond M, Rousset F (1995) GENEPOP (Version 1.2): Population Genetics
19 Software for Exact Tests and Ecumenicism. *J Hered* 3:248–249
- 20 Rice WER (1989) Analyzing tables of statistical tests. *Evolution* (N Y) 43:223–225.
- 21 Ryman N, Palm S (2006) POWSIM: a computer program for assessing statistical

- 1 power when testing for genetic differentiation. *Mol Ecol* 6:600–602.
- 2 Sánchez-Velasco L, Lavín MF, Jiménez-Rosenberg S. . A, et al (2013) Three-
3 dimensional distribution of fish larvae in a cyclonic eddy in the Gulf of
4 California during the summer. *Deep Res Part I Oceanogr Res Pap* 75:39–51.
- 5 Santiago-García MW, Marinone SG, Velasco-Fuentes OU (2014) Three-
6 dimensional connectivity in the Gulf of California based on a numerical model.
7 *Prog Oceanogr* 123:64–73.
- 8 Schuelke M (2000) An economic method for the fluorescent labeling of PCR
9 fragments. *Nat Biotechnol* 18:233–234.
- 10 Selkoe, K. A., D’Aloia, C. C., Crandall, E. D., Iacchei, M., Liggins, L., Puritz, J. B.,
11 von der Heyden, S., et al. 2016. A decade of seascape genetics: Contributions
12 to basic and applied marine connectivity. *Marine Ecology Progress Series*,
13 554: 1-19.
- 14 Slatkin M (1985) Rare Alleles as Indicators of Gene Flow. *Evolution* (N Y) 39:53–
15 65
- 16 Soria G, Munguía-Vega a., Marinone SG, et al (2012) Linking bio-oceanography
17 and population genetics to assess larval connectivity. *Mar Ecol Prog Ser*
18 463:159–175.
- 19 Stobutzki IC, Bellwood DR (1997) Sustained swimming abilities of the late pelagic
20 stages of coral reef fishes. *Mar Ecol Prog Ser* 149:35–41
- 21 Teske PR, Sandoval-Castillo J, van Sebille E, et al (2016) Oceanography promotes

- 1 self-recruitment in a planktonic larval disperser. *Sci Rep* 6:1–8.
- 2 Tinhan T, Erisman B, Aburto-Oropeza O, et al (2014) Residency and seasonal
3 movements in *Lutjanus argentiventris* and *Mycteroperca rosacea* at Los
4 Islotes Reserve, Gulf of California. *Mar Ecol Prog Ser* 501:191–206.
- 5 Trembl EA, Halpin PN, Urban DL, Pratson LF (2008) Modeling population
6 connectivity by ocean currents, a graph-theoretic approach for marine
7 conservation. *Landsc Ecol* 23:19–36.
- 8 Untergasser A, Cutcutache I, Koressaar T, et al (2012) Primer3-new capabilities
9 and interfaces. *Nucleic Acids Res* 40:1–12.
- 10 Valadez-Rodríguez JA (2017) Caracterización de microsatélites en el pargo
11 lunarejo, *Lutjanus guttatus*. B.S. dissertation. Tecnológico Nacional de México:
12 Instituto Tecnológico de la Paz, B.C.S.
- 13 Van Oosterhout C, Hutchinson WF, Wills DPM, Shipley P (2004) MICRO-
14 CHECKER: Software for identifying and correcting genotyping errors in
15 microsatellite data. *Mol Ecol Notes* 4:535–538.
- 16 Waples RS (1998) Separating the wheat from the chaff: Patterns of genetic
17 differentiation in high gene flow species. *J Hered* 89:438–450.
- 18 Waples RS, Gaggiotti O (2006) What is a population? An empirical evaluation of
19 some genetic methods for identifying the number of gene pools and their
20 degree of connectivity. *Mol Ecol* 15:1419–1439.
- 21 Weir B. S., Cockerham C. (1984) Estimating F-Statistics for the Analysis of

1 Population. Evolution (N Y) 38:1358–1370

2 Zapata FA, Herrón PA (2002) Pelagic larval duration and geographic distribution of
3 tropical eastern Pacific snappers (Pisces : Lutjanidae). Mar Ecol Prog Ser
4 230:295–300.

5 Zavala-Sansón L (2015) Surface dispersion in the Gulf of California. Prog
6 Oceanogr 137:24–37.

Figure caption:

7 **Fig. 1** Study area in the Southern Gulf of California. The gray triangles indicate the
8 genetic sampling site and black dots represent the location of larval release sites
9 within each spatial unit of analysis (squares). Locations on the peninsular coast
10 include San Jose (SJ), Francisquito (F), Espiritu Santo (ES), Gaviota (G), Cetmar
11 (C), and Mogote (M). Locations on mainland coast include Topolobampo (T),
12 Huitusi (H), and Altata (A)

13 **Fig. 2** Mean of the estimators of genetic diversity. The gray bars are the number of
14 alleles (N_a), the white bars are the effective alleles (N_e) and the black bars are the
15 private alleles. The black triangles and gray crosses are the expected (H_e) and
16 observed (H_o) heterozygosities, respectively. Locations on the peninsular side
17 include Espiritu Santo (ES), San Jose (SJ), Gaviota (G), Francisquito (F), Mogote
18 (M), Cetmar (C). Locations on mainland side include Topolobampo (T), Huitusi (H),
19 and Altata (A)

20 **Fig. 3** Mean relatedness coefficient between individuals in the same locality (r).
21 Black dots represent the 95% confidence interval of the null hypothesis of random

1 mating within the same locality. Locations on the peninsular side include Espiritu
2 Santo (ES), San Jose (SJ), Gaviota (G), Francisquito (F), Mogote (M), Cetmar (C).
3 Locations on mainland side include Topolobampo (T), Huitusi (H), and Altata (A).
4 The p -values for each locality were: IES = 0.008, ISJ = 0.05, IG = 0.22, SF = 0.1,
5 Mo = 0.8, Cet = 0.14, Topo = 0.46, Hu = 0.36 y Alt = 0.2

6 **Fig. 4** Climatology of circulation (1985-2005) for a) June, c) July, and e) August,
7 and connectivity matrices for a pelagic larval duration of 20 days for b) June, d)
8 July, and f) August. In the matrices, the X axes represent the origin quadrant and
9 the Y axes the destination quadrant. The colored bar represents the most probable
10 arrival days. The quadrants 6, 8, 9, 15, 17 and 22 are represented with genetic
11 data (yellow triangles)

12 **Fig. 5** Spatial network from first generation migrants estimated from the genetic
13 data. The width of the lines are scaled according to the number of migrants. Colors
14 show the direction: a) southward and eastward, b) northward and westward.
15 Populations include San Jose - Francisquito (SJ-F), Espiritu Santo - Gaviota (ES-
16 G), Mogote - Cetmar (M-C), Topolobampo (T), Huitusi (H), Altata (A)

17 **Fig.6** Spatial network from the connectivity matrices showing the probability of
18 larval dispersal according to the oceanographic ROMS model in a window of time
19 between 15 and 20 days: a) June, b) July and c) August. The width of the lines are
20 scaled according to the probability. Colors show the direction. Populations include
21 San Jose and Francisquito (SJ-F), Espiritu Santo and Gaviota (ES-G), Cetmar and
22 Mogote (C-M), Topolobampo (T), Huitusi (H) and Altata (A)

1 **Table caption:**

2 **Table 1** Sample sizes collected for genetic analyses, size range and stage of

3 *Lutjanus argentiventris* at six locations in the peninsular coast and three locations

4 in the mainland coast of the Southern Gulf of California

5 **Table 2** Paired F_{ST} values between locations (below the diagonal) and p -values

6 (above the diagonal). Locations on the peninsular coast include Espiritu Santo

7 (ES), San Jose (SJ), Gaviota (G), Francisquito (F), Mogote (M), and Cetmar (C).

8 Locations on the mainland coast include Topolobampo (T), Huitusi (H), and Altata

9 (A)

10 **Table 3** Estimation of Number of migrants (Nm) based on private alleles within

11 each location

12 **Table 4** Number of inbound (in-degree) and outbound (out-degree) connections,

13 estimated from the first generation migrants

14 **Table 5** Number of inbound (in-degree) and outbound (out-degree) connections

15 estimated from the modelled connectivity networks for the sites with genetic data

16 **Table 6** Highest natural log of Bayes factor (probability) with Bezier approximation

17 for each gene flow model estimated with Migrate-n for two sets of runs (narrow and

18 wide priors, respectively) using the genotypes for six populations and 12

19 microsatellites markers for *L. argentiventris*. One replicate shown

20 **Table 7** Mean mutation-scaled effective population size (Θ), number of migrants

21 entering each site (In), number of migrants leaving each site (out), and sink and

22 source sites (Out-In). The negative values represent net sinks and positive values

23 net sources

Fig. 1

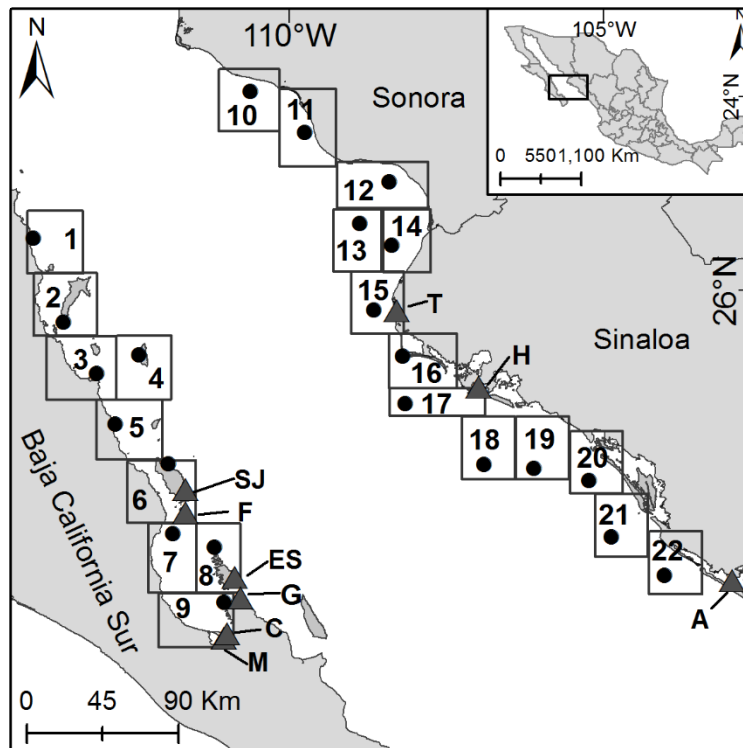


Fig. 2

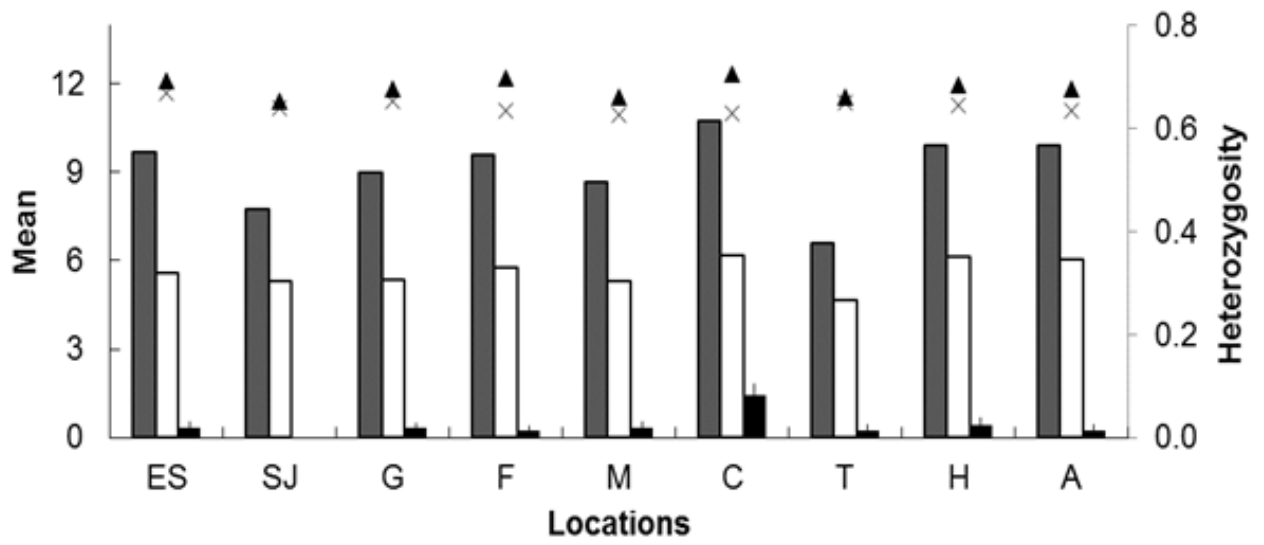


Fig. 3

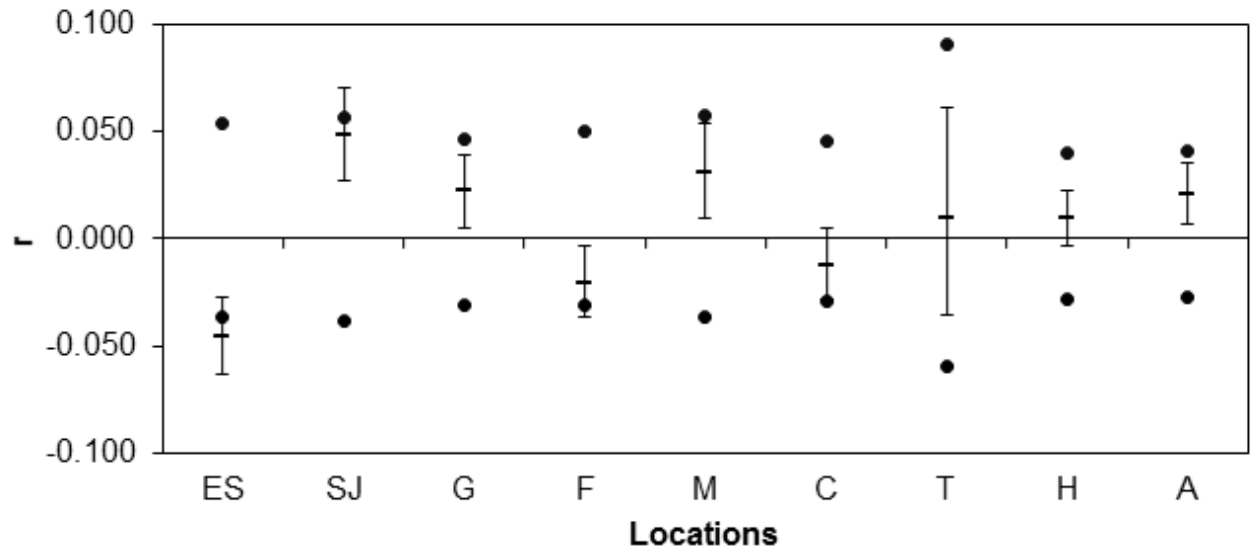


Fig. 4

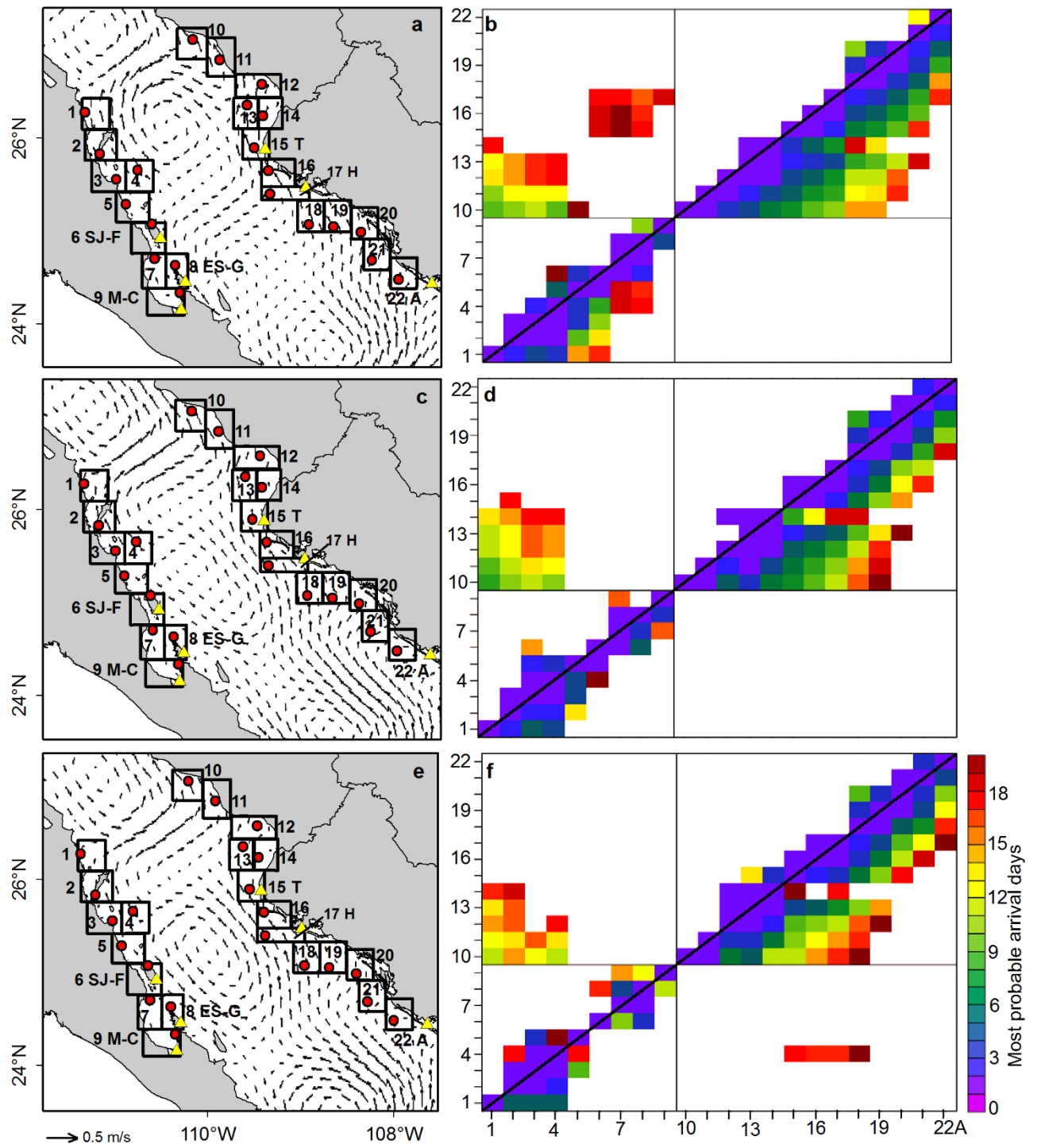


Fig. 5

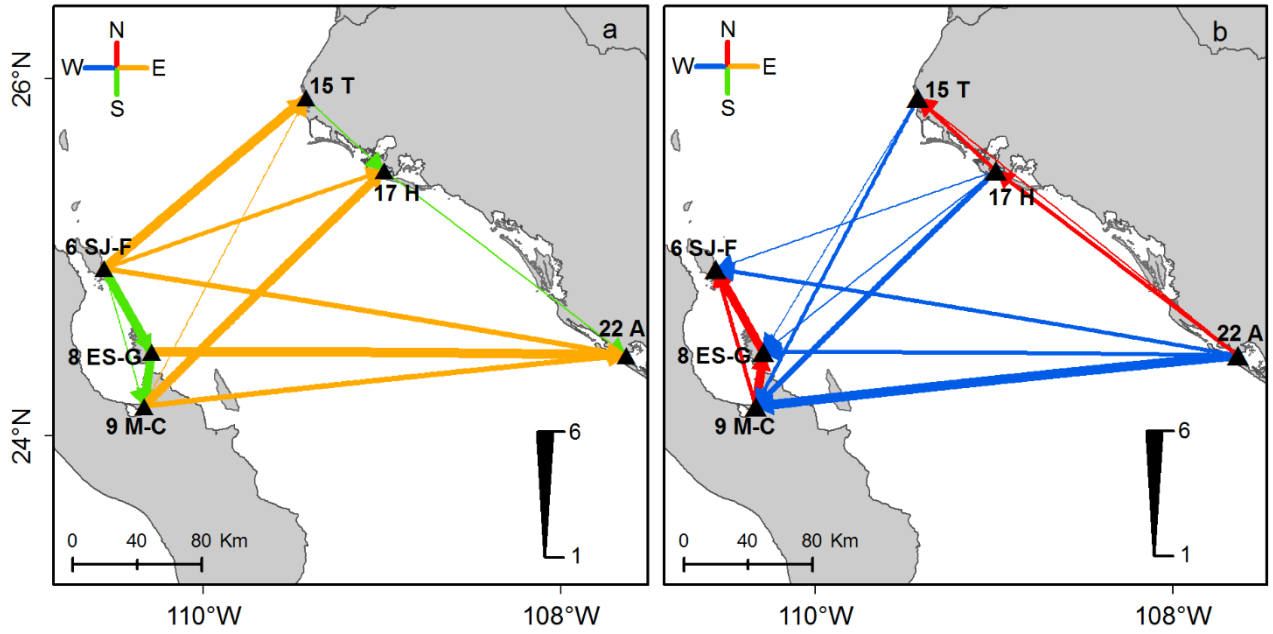


Fig. 6

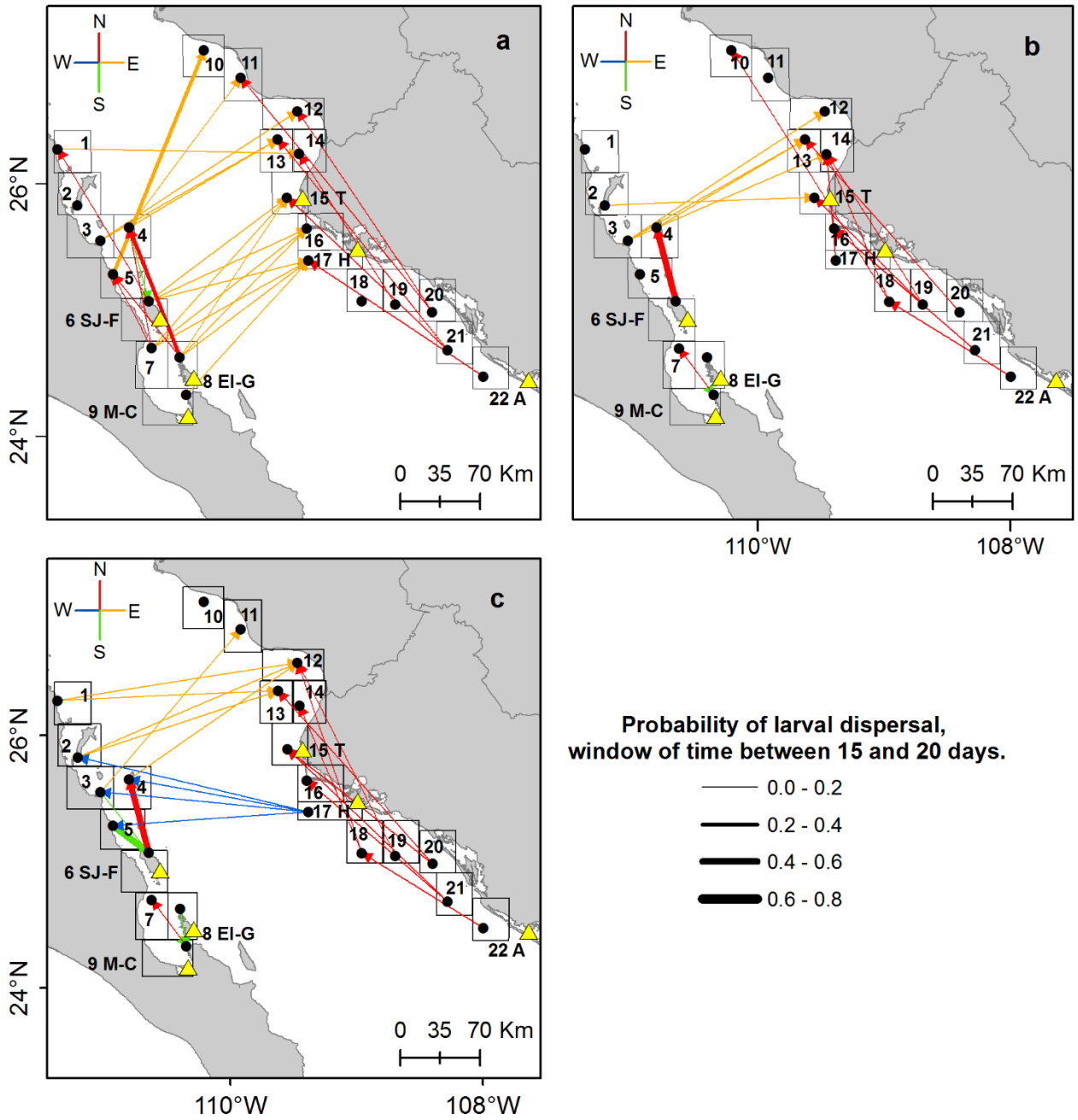


Table 1

Location	Sample size	Size range (cm)	% juvenile / %adults	Collection date
Peninsular coast				
San Jose	20	7 – 19.5	100 / 0	May-August 2015
Francisquito*	26	>32	0 / 100	May-August 2015
Espiritu Santo	32	20.7 – 35.3	92 / 8	December 2015
Gaviota	27	8 - 19	100 / 0	May-August 2015
Mogote	20	6 – 18	100 / 0	May 2015
Cetmar	32	2.8 - 8	100 / 0	September 2015
Mainland coast				
Topolobampo	12	12.5 – 27.2	100 / 0	August 2016
Huitusi	32	9.5 – 28.9	100 / 0	August 2016
Altata	32	13.9 – 19.5	100 / 0	August 2016

*There is no specific size range, but all the specimens were of commercial size.

Table 2

	Peninsula						Mainland		
	ES	SJ	G	F	M	C	T	H	A
ES	-	0.54	0.76	0.97	0.74	0.73	0.59	0.77	0.88
SJ	-0.0002	-	0.89	0.49	0.49	0.47	0.91	0.80	0.28
G	-0.0023	-0.0047	-	0.33	0.28	0.20	0.39	0.68	0.32
F	-0.0059	0.0014	0.0031	-	0.63	0.95	0.89	0.91	0.07
M	-0.0023	0.0008	0.0035	0.0003	-	0.18	0.07	0.54	0.32
C	-0.0011	0.0015	0.0046	-0.0038	0.0062	-	0.75	0.96	0.10
T	-0.0006	-0.0086	0.0032	-0.0056	0.0158	-0.0021	-	0.81	0.12
H	-0.0021	-0.0027	-0.0010	-0.0035	0.0005	-0.0042	-0.0041	-	0.47
A	-0.0034	0.0033	0.0025	0.0085	0.0032	0.0064	0.0113	0.0010	-

$p > 0.06$

Table 3

Location	<i>Nm</i>
Espiritu Santo	13.409
Gaviota	5.053
Francisquito	18.447
Mogote	6.593
Cetmar	17.083
Peninsula	11.983
Topolobampo	3.006
Huitusi	13.463
Altata	28.243
Mainland	9.027

Table 4

	Location	In-degree	Out-degree
Peninsular coast	San Jose - Francisquito	4	5
	Espiritu Santo - Gaviota	5	3
	Mogote- Cetmar	5	5
	Sum	14	13
	Mean	4.6	4.3
Mainland coast	Topolobampo	4	3
	Huitusi	4	5
	Altata	4	5
	Sum	12	13
	Mean	4	4.3

Table 5

Locality	June		July		August		Sum	
	In-degree	Out-degree	In-degree	Out-degree	In-degree	Out-degree	In-degree	Out-degree
San Jose - Francisquito	1	4	0	1	0	1	1	6
Espiritu Santo - Gaviota	0	5	0	0	1	0	1	5
Cetmar - Mogote	0	1	1	1	0	0	1	2
Topolobampo	4	0	2	0	2	2	8	2
Huitusi	3	0	2	0	1	1	6	1
Altata	5	0	0	1	1	3	6	4
Sum	13	10	5	3	5	7	23	20

Table 6

Model No.	Bezier approximation	Rank	Probability
1 Panmictic	-5474519.63	5	0
2 Full model	-2264751.53	1	1
3 June oceanograhly	-2876054.15	2	0
4 July oceanography	-3752178.05	4	0
5 August oceanography	-2897148.14	3	0

Table 7

	Locality	Mean Θ	In	Out	Out-In
Peninsular coast	Espiritu Santo - Gaviota	0.0979	9.0902	16.9419	7.8518
	San Jose - Francisquito	0.0979	6.0467	8.4710	2.4243
	Cetmar-Mogote	0.0981	15.4831	18.2801	2.7970
Continental coast	Topolobampo	0.0972	9.6603	6.8793	-2.7810
	Huitusi	0.0978	17.5962	8.7006	-8.8956
	Altata	0.0972	6.5380	5.1415	-1.3965

Reguera-Rouzaud Nicole¹, Díaz-Viloria Noe^{1*}, Sánchez-Velasco Laura¹, Flores-Morales Ana Laura², Parés-Sierra Alejandro³, Aburto-Oropeza, Octavio⁴, Munguía-Vega Adrián^{5, 6}

Yellow snapper (*Lutjanus argentiventris*) connectivity in the Southern Gulf of California

¹Instituto Politécnico Nacional–Centro Interdisciplinario de Ciencias Marinas (IPN-CICIMAR), Departamento de Plancton y Ecología Marina, La Paz, B.C.S., 23096, Mexico.

²Departamento de Oceanografía Física, Facultad de Ciencias Marinas, Universidad Autónoma de Baja California, Ensenada, B.C., 22860, Mexico.

³Departamento de Oceanografía Física, Centro de Investigación Científica y de Educación Superior de Ensenada, Ensenada, B.C., 22860, Mexico.

⁴Marine Biology Research Division, Scripps Institution of Oceanography, University of California, San Diego, La Jolla, CA 92093-0202, USA.

⁵Conservation Genetics Laboratory, School of Natural Resources and the Environment, University of Arizona, Tucson, AZ, 85721, USA

⁶@ Lab Applied Genetics Consultancy. La Paz, Baja California Sur, 23000, Mexico

*Corresponding author: Tel. +52 (612) 122-5366, Ext. 81567; Fax: +52 (612) 122-5322, ndviloria@hotmail.com

Electronic supplementary material

S1. Characterization of 18 microsatellites loci in a sample of *Lutjanus argentiventris* from Espiritu Santo. Locus name, GenBank accession number (in bold), forward (F) and reverse (R) primers, fluorescent dye employed, allelic size range, sample size (N), number of alleles per locus (N_a), observed (H_o) and expected (H_e) heterozygosities, inbreeding coefficient (F_{IS}), p value for Hardy-Weinberg Equilibrium (p) and null allele frequencies (NaF). Underlined loci were used in subsequent population genetic analyses.

Locus	Repeat motif	Primer sequence (5'-3')	Dye label	Allelic size range (bp)	N	N_a	H_o	H_e	F_{IS}	p	NaF
<u>Larg1</u>	(CA) ₁₇	F: ACACTGAGCGGAGGCAAG R: GCTGGATTTGCATTGAGTGA	FAM	188-219	31	14	0.903	0.872	-0.019	0.925	-0.017
KY606690											
<u>Larg4</u>	(CA) ₁₂	F: AATGATCACTCCGTGTGTGC R: CTGCTGTATTTTCCGGCTGT	FAM	239-261	28	10	0.786	0.865	0.109	0.504	0.042
KY606691											
<u>Larg5</u>	(CA) _{9..}	F: AGGGTCAGAGGTCAGGAGGT R: GCGCTTCACACAGCTGTTAC	FAM	229-282	28	17	0.857	0.863	0.025	0.629	0.003
KY606692	(CA) ₁₇										
Larg7	(CA) ₂₁	F: TCCCTGTGGAACCTCTCCTG R: TTGTCATTGCAGGCCAAATA	FAM	205-278	28	19	0.357	0.922	0.587	0.000*	0.294
KY606693											
<u>Larg11</u>	(CA) ₁₀	F: CAATAAGGGGGCAGAATGTG R: CCTGTAATGCGTGTCTGCAT	FAM	213-228	29	5	0.655	0.659	0.024	0.990	0.002
KY606694											
<u>Larg19</u>	(GT) ₂₉	F: CACAAGAGGCACCTGTAGCA R: ACAGGCTGTTTCCCAGAGTC	FAM	449-483	24	6	0.625	0.575	-0.066	0.143	-0.032
KY606695											

S1. Continued.

Locus	Repeat motif	Primer sequence (5'-3')	Dye label	Allelic size range (bp)	<i>N</i>	<i>Na</i>	<i>Ho</i>	<i>He</i>	<i>F_{IS}</i>	<i>P</i>	<i>NaF</i>
<u>Larg27</u>	(CCT) ₈	F: TGTCTGTAGGGGGAGTGAG	FAM	149-171	31	8	0.645	0.652	0.027	0.695	0.004
KY606696		R: GTGGCGGTGGAATATGAAAC									
<u>Lupe39^a</u>	(AC) ₃₉	F: CCTTTCATCAGAGCAGAGGC	PET	213-283	32	24	0.938	0.943	0.022	0.832	0.003
KU951507		R: CATGTGCACGTTCACTCTCC									
Lupe55 ^a	(GT) ₃₃	F: GACTGTACCATGTTCGAGGGG	VIC	226-260	32	13	0.781	0.849	0.096	0.026	0.037
KU951516		R: TTGTGCAGGATACGTGCTGT									
<u>Lupe62^a</u>	(GT) ₃₁	F: TGGGAATTAGTGACTGTGAGCA	NED	232-239	32	4	0.375	0.409	0.098	0.045	0.024
KU951519		R: GAGCACGACAGCATTAGCAG									
<u>Lupe1^a</u>	(GAGT) ₃₈	F: AACTTTGCAGAACCGAGGAG	PET	110-128	32	5	0.500	0.518	0.051	0.107	0.012
KU951491		R: TTTGAGATTAGCTGCGGACA									
Lupe24 ^a	(AGAT) ₁₃	F: GCTCAACATGAAGGGCTGAT	FAM	229-288	32	16	0.625	0.912	0.329	0.000*	0.150
KU951499		R: GCCTGTGACCCCATATAACC									
<u>Lupe29^a</u>	(AGAT) ₁₁	F: CGGACATTCATAATAGAACAACAGA	PET	117-134	31	4	0.194	0.181	-0.056	1.000	-0.011
KU951502		R: CTGCAGTGAGCTGAGCTTTT									
Lupe33 ^a	(TGGA) ₁₁	F: CGGACATTCATAATAGAACAACAGA	VIC	113-199	27	13	0.556	0.870	0.377	0.000*	0.168
KU951503		R: CTGCAGTGAGCTGAGCTTTT									
<u>Lupe34^a</u>	(AGAT) ₁₀	F: CTGACTTTCACCTCATGACAGA	VIC	222-339	31	22	0.871	0.928	0.078	0.226	0.030
KU951504		R: GTTAGGGTAAGGGAGGGCAG									

S1. Continued.

Locus	Repeat motif	Primer sequence (5'-3')	Dye label	Allelic size range (bp)	<i>N</i>	<i>N_a</i>	<i>H_o</i>	<i>H_e</i>	<i>F_{IS}</i>	<i>P</i>	<i>NaF</i>
<u>Lgut19</u> ^b	(ATCT) ₁₈	F: TGAATCAGCGACTCTGACAGC	FAM	287-316	30	8	0.867	0.837	-0.019	0.419	-0.016
MF416124		R: ACCCAGACTGGCTGTGCC									
<u>Lgut26</u> ^b	(ATCT) ₁₈	F: AAAC TTGGTACACAGCTTCTCCG	NED	200-259	31	15	0.774	0.906	0.161	0.000*	0.069
MF416126		R: ACATCTGTTGCTGCCACTGC									
<u>Lgut21</u> ^b	(ATCT) ₁₈	F: AAGGAGGACTTTATTCCATCAGC	FAM	252-373	27	20	0.704	0.933	0.264	0.000*	0.119
MF416125		R: GGGGACAGTTGGTTCATCC									

*, Significant departures of Hardy-Weinberg Equilibrium ($p < 0.004$), after sequential Bonferroni test. ^a, microsatellites isolated from *L. peru* (Paz-García et al. 2017); ^b, microsatellites isolated from *L. guttatus* (Valadez-Rodriguez, 2017).

S2. Genetic diversity indexes per locus and location. Sample size (N), average number of alleles per locus (Na), average effective number of alleles (Ne), average observed (Ho) and expected (He) heterozygosities, p values for Hardy-Weinberg Equilibrium (p) and null allele frequencies (NaF). Locations on the peninsular coast: Espiritu Santo (ES), San Jose(SJ), Gaviota (G), Francisquito (F), Mogote (M), Cet-mar (C). Locations on continental coast: Topolobampo (T), Huitusi (H), and Altata (A).

Locus		Locations								
		ES	SJ	G	F	M	C	T	H	A
Larg01	<i>N</i>	23	20	26	25	19	30	10	31	31
	<i>Na</i>	14	12	12	13	11	17	9	13	16
	<i>Ne</i>	9.532	8.421	7.511	7.396	7.078	9.278	6.452	8.619	9.806
	<i>Ho</i>	1.000	0.750	1.000	0.760	0.895	0.900	1.000	0.871	0.903
	<i>He</i>	0.895	0.881	0.867	0.865	0.859	0.892	0.845	0.884	0.898
	<i>p</i>	0.994	0.145	0.690	0.042	0.765	0.439	0.306	0.295	0.578
	<i>NaF</i>	-0.055	0.070	-0.071	0.056	-0.021	-0.004	-0.084	0.007	-0.003
Larg04	<i>N</i>	22	20	26	25	19	30	10	30	31
	<i>Na</i>	10	8	11	12	10	11	8	9	11
	<i>Ne</i>	7.278	5.333	7.153	7.716	6.119	6.923	6.452	6.498	6.180
	<i>Ho</i>	0.818	0.850	0.654	0.800	0.684	0.833	0.900	0.667	0.903
	<i>He</i>	0.863	0.813	0.860	0.870	0.837	0.856	0.845	0.846	0.838
	<i>p</i>	0.884	0.732	0.030	0.073	0.096	0.341	0.713	0.368	0.922
	<i>NaF</i>	0.024	-0.021	0.111	0.038	0.100	0.012	-0.030	0.097	-0.035
Larg05	<i>N</i>	22	20	26	24	19	29	10	31	31
	<i>Na</i>	16	10	13	16	17	18	7	17	17
	<i>Ne</i>	6.497	6.061	5.323	6.128	7.078	5.760	5.714	8.430	10.116
	<i>Ho</i>	0.818	0.700	0.846	0.750	0.842	0.759	1.000	0.710	0.774
	<i>He</i>	0.846	0.835	0.812	0.837	0.859	0.826	0.825	0.881	0.901
	<i>p</i>	0.687	0.269	0.922	0.252	0.763	0.183	0.258	0.041	0.136
	<i>NaF</i>	0.015	0.074	-0.019	0.047	0.010	0.037	-0.096	0.091	0.067

S2. Continued.

Locus		Locations								
		ES	SJ	G	F	M	C	T	H	A
Larg11	<i>N</i>	23	19	26	25	19	30	10	28	31
	<i>Na</i>	5	3	5	4	5	6	3	4	5
	<i>Ne</i>	2.619	2.022	2.625	2.588	2.911	3.000	1.852	2.501	2.734
	<i>Ho</i>	0.609	0.632	0.462	0.720	0.632	0.633	0.300	0.429	0.645
	<i>He</i>	0.618	0.506	0.619	0.614	0.657	0.667	0.460	0.600	0.634
	<i>p</i>	0.975	0.846	0.044	0.865	0.075	0.034	0.169	0.138	0.791
	<i>NaF</i>	0.006	-0.084	0.097	-0.066	0.019	0.020	0.110	0.107	-0.007
Larg19	<i>N</i>	18	20	26	25	19	29	10	31	31
	<i>Na</i>	5	2	3	3	2	5	2	3	3
	<i>Ne</i>	2.348	1.923	2.039	2.159	1.819	2.184	1.980	2.000	1.975
	<i>Ho</i>	0.611	0.700	0.615	0.280	0.474	0.448	0.300	0.645	0.323
	<i>He</i>	0.574	0.480	0.510	0.537	0.450	0.542	0.495	0.500	0.494
	<i>p</i>	0.121	0.076	0.486	0.002	1.000	0.026	0.246	0.324	0.034
	<i>NaF</i>	-0.024	-0.149	-0.070	0.167	-0.026	0.061	0.130	-0.097	0.115
Lupe39	<i>N</i>	23	19	24	25	19	29	10	31	30
	<i>Na</i>	19	18	22	21	19	25	14	28	27
	<i>Ne</i>	13.225	13.127	13.714	14.205	15.042	19.114	10.000	17.963	17.822
	<i>Ho</i>	0.826	0.895	0.833	0.880	0.632	0.759	1.000	0.903	0.900
	<i>He</i>	0.924	0.924	0.927	0.930	0.934	0.948	0.900	0.944	0.944
	<i>p</i>	0.242	0.247	0.028	0.513	0.000*	0.000*	1.000	0.024	0.441
	<i>NaF</i>	0.051	0.015	0.049	0.026	0.193	0.097	-0.053	0.021	0.023

S2. Continued.

Locus		Locations								
		ES	SJ	G	F	M	C	T	H	A
Lupe62	N	23	20	26	25	17	30	10	29	31
	Na	4	3	4	4	4	6	4	3	4
	Ne	1.906	1.766	1.559	2.260	1.736	1.875	2.041	1.644	1.440
	Ho	0.435	0.250	0.192	0.280	0.412	0.533	0.400	0.379	0.258
	He	0.475	0.434	0.359	0.558	0.424	0.467	0.510	0.392	0.305
	p	0.085	0.002	0.003	0.000*	0.075	0.561	0.305	1.000	0.007
	NaF	0.028	0.128	0.123	0.178	0.015	-0.046	0.073	0.009	0.036
Larg27	N	23	20	26	25	19	30	10	31	31
	Na	8	4	6	6	6	6	3	4	6
	Ne	2.899	1.606	2.406	2.319	2.256	2.442	1.852	1.864	2.633
	Ho	0.609	0.450	0.538	0.600	0.579	0.300	0.600	0.419	0.613
	He	0.655	0.378	0.584	0.569	0.557	0.591	0.460	0.464	0.620
	p	0.525	1.000	0.147	0.940	0.719	0.000*	1.000	0.317	0.760
	NaF	0.028	-0.053	0.029	-0.020	-0.020	0.183	-0.096	0.030	0.005
Lupe01	N	23	20	26	25	19	30	10	31	31
	Na	5	4	4	4	3	5	4	4	3
	Ne	2.213	2.446	2.908	2.495	2.034	2.830	3.279	2.921	1.768
	Ho	0.478	0.550	0.731	0.440	0.368	0.500	0.300	0.548	0.355
	He	0.548	0.591	0.656	0.599	0.508	0.647	0.695	0.658	0.434
	p	0.131	0.663	0.869	0.059	0.022	0.017	0.001	0.128	0.020
	NaF	0.045	0.026	-0.045	0.100	0.160	0.089	0.233	0.066	0.056
Lupe29	N	23	20	26	25	19	23	10	31	30
	Na	3	2	2	2	3	2	3	4	2

S2. Continued.

Locus	Locations									
	ES	SJ	G	F	M	C	T	H	A	
	<i>Ne</i>	1.193	1.280	1.166	1.268	1.112	1.293	1.227	1.349	1.427
	<i>Ho</i>	0.174	0.150	0.154	0.240	0.105	0.261	0.200	0.226	0.167
	<i>He</i>	0.162	0.219	0.142	0.211	0.101	0.227	0.185	0.259	0.299
	<i>p</i>	1.000	0.246	1.000	1.000	1.000	1.000	1.000	0.506	0.032
	<i>NaF</i>	-0.011	0.056	-0.010	-0.024	-0.020	-0.028	-0.013	0.026	0.102
Lupe34	<i>N</i>	23	19	26	25	18	30	10	31	31
	<i>Na</i>	18	16	17	20	15	16	14	20	16
	<i>Ne</i>	11.756	12.237	11.556	13.587	9.818	11.688	10.000	12.481	10.560
	<i>Ho</i>	0.826	0.947	0.962	0.880	1.000	0.800	1.000	0.968	0.903
	<i>He</i>	0.915	0.918	0.913	0.926	0.898	0.914	0.900	0.920	0.905
	<i>p</i>	0.204	0.350	0.669	0.142	0.132	0.126	1.000	0.368	0.464
	<i>NaF</i>	0.046	-0.015	-0.025	0.024	-0.054	0.060	-0.053	-0.025	0.001
Lgut19	<i>N</i>	23	19	26	25	19	30	10	31	31
	<i>Na</i>	9	11	9	10	9	12	8	10	9
	<i>Ne</i>	5.781	7.367	6.500	6.906	6.446	7.895	4.878	6.939	6.102
	<i>Ho</i>	0.826	0.789	0.846	0.960	0.895	0.800	0.800	0.935	0.871
	<i>He</i>	0.827	0.864	0.846	0.855	0.845	0.873	0.795	0.856	0.836
	<i>p</i>	0.220	0.033	0.556	0.708	0.640	0.188	0.707	0.316	0.989
	<i>NaF</i>	0.001	0.040	0.000	-0.057	-0.029	0.039	-0.003	-0.043	-0.019
Mean	<i>N</i>	22	20	26	25	19	29	10	31	31
	<i>Na</i>	9.667	7.750	9.000	9.583	8.667	10.750	6.583	9.917	9.917
	<i>Ne</i>	5.604	5.299	5.372	5.752	5.287	6.190	4.644	6.101	6.047
	<i>Ho</i>	0.669	0.639	0.653	0.633	0.626	0.627	0.650	0.642	0.635

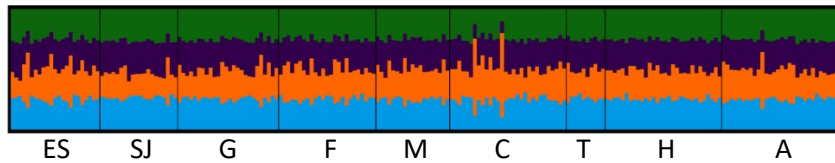
S2. Continued.

Locus	Locations									
	ES	SJ	G	F	M	C	T	H	A	
<i>He</i>	0.692	0.653	0.675	0.698	0.661	0.704	0.660	0.684	0.676	
<i>p</i>	0.506	0.384	0.454	0.418	0.481	0.291	0.559	0.319	0.431	
<i>NaF</i>	0.013	0.007	0.014	0.039	0.027	0.043	0.010	0.024	0.028	

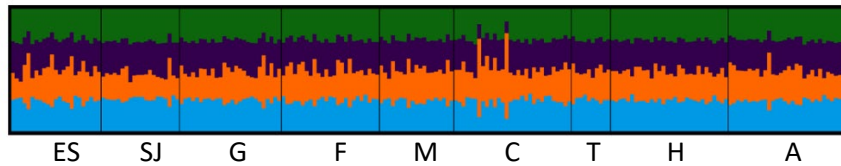
*** $p < 0.0005$**

S3. Summary plot of estimates of Q (average membership coefficient). Each individual is represented by a single vertical line broken into K colored segments. K= 4 10/10, Mean (LnProb)= -9505.370, Mean (similarity score) = 0.989. Locations on the peninsular coast: Espiritu Santo (ES), San Jose(SJ), Gaviota (G), Francisquito (F), Mogote (M), Cet-mar (C). Locations on continental coast: Topolobampo (T), Huitusi (H), and Altata (A).

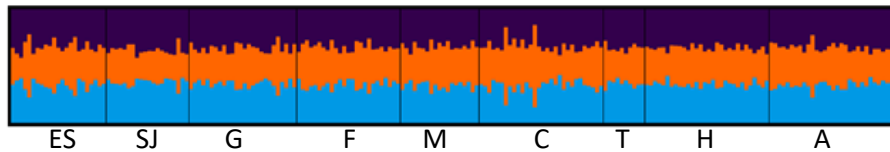
Replicate 1: Mean (LnProb)= -9505.370, Mean (similarity score) = 0.989



Replicate 2: Mean (LnProb) = -9484.530, Mean (similarity score) = 0.988



Replicate 3: Mean (LnProb) = -9359.450, Mean (similarity score) = 0.993



S4. Highest natural log of Bayes factor (probability) with Bezier approximation for the three replicates for each gene flow model estimated with Migrate-n using the genotypes for six populations and 12 microsatellites markers for *L. argentiventris*.

Model No.	Bezier approximation	Rank	Probability
1 Panmictic R1	-5474519.63	14	0
1 Panmictic R2	-5477115.37	15	0
1 Panmictic R3	-5472830.99	13	0
2 Full model R1	-2264751.53	1	1
2 Full model R2	-2267387.04	2	0
2 Full model R3	-2268932.98	3	0
3 June oceanography R1	-2876054.15	6	0
3 June oceanography R2	-2856494.13	5	0
3 June oceanography R3	-2851756.13	4	0
4 July oceanography R1	-3752178.05	11	0
4 July oceanography R2	-3743699.27	10	0
4 July oceanography R3	-3762217.81	12	0
5 August oceanography R1	-2897148.14	7	0
5 August oceanography R2	-2941180.07	8	0
5 August oceanography R3	-3042766.90	9	0

S5. Number of migrants per generations (Nm) for all loci. Θ is the mutation-scaled effective population size for the recipient populations and M the mutation-scaled migration rate. Locations on the peninsular coast: Espiritu Santo-Gaviota (ES-G), San Jose-Francisquito (SJ-F), Mogote-Cet-mar (M-C). Locations on continental coast: Topolobampo (T), Huitusi (H), and Altata (A).

Locus	Parameter	Mean	$Nm = \Theta^*(M/4)$
All	Θ_{ES-G}	0.098	
All	Θ_{SJ-F}	0.098	
All	Θ_{M-C}	0.098	
All	Θ_T	0.097	
All	Θ_H	0.098	
All	Θ_A	0.097	
All	$M_{SJ-F \text{ to } ES-G}$	61.539	1.506
All	$M_{M-C \text{ to } ES-G}$	62.348	1.526
All	$M_T \text{ to } ES-G$	96.820	2.369
All	$M_H \text{ to } ES-G$	119.470	2.923
All	$M_A \text{ to } ES-G$	31.305	0.766
All	$M_{ES-G \text{ to } SJ-F}$	41.647	1.019
All	$M_{M-C \text{ to } SJ-F}$	90.350	2.211
All	$M_T \text{ to } SJ-F$	38.055	0.931
All	$M_H \text{ to } SJ-F$	32.063	0.785
All	$M_A \text{ to } SJ-F$	44.965	1.100
All	$M_{ES-G \text{ to } M-C}$	394.239	9.670
All	$M_{SJ-F \text{ to } M-C}$	102.973	2.526
All	$M_T \text{ to } M-C$	33.311	0.817
All	$M_H \text{ to } M-C$	54.780	1.344
All	$M_A \text{ to } M-C$	45.952	1.127
All	$M_{ES-G \text{ to } T}$	121.048	2.942
All	$M_{SJ-F \text{ to } T}$	94.204	2.290
All	$M_{M-C \text{ to } T}$	37.796	0.919
All	$M_H \text{ to } T$	106.004	2.577
All	$M_A \text{ to } T$	38.368	0.933
All	$M_{ES-G \text{ to } H}$	64.649	1.581
All	$M_{SJ-F \text{ to } H}$	37.245	0.911
All	$M_{M-C \text{ to } H}$	505.194	12.351
All	$M_T \text{ to } H$	62.954	1.539
All	$M_A \text{ to } H$	49.711	1.215
All	$M_{ES-G \text{ to } A}$	71.229	1.730
All	$M_{SJ-F \text{ to } A}$	51.010	1.239
All	$M_{M-C \text{ to } A}$	52.447	1.274
All	$M_T \text{ to } A$	50.338	1.223
All	$M_H \text{ to } A$	44.140	1.072